Cellular Signalling 61 (2019) 93–107

Contents lists available at ScienceDirect

Cellular Signalling

journal homepage: www.elsevier.com/locate/cellsig

The interaction between PLEKHG2 and ABL1 suppresses cell growth via the NF-κB signaling pathway in HEK293 cells

Masashi Nishikawa[a], Shun Nakano[a], Hiromu Nakao[b], Katsuya Sato[c], Tsuyoshi Sugiyama[d], Yukihiro Akao[a], Hitoshi Nagaoka[c], Hisashi Yamakawa[e], Takahiro Nagase[e], Hiroshi Ueda[a,b,*]

[a] United Graduate School of Drug Discovery and Medical Information Sciences, Gifu University, Yanagido 1-1, Gifu 501-1193, Japan
[b] Department of Chemistry and Biomolecular Science, Faculty of Engineering, Gifu University, Yanagido 1-1, Gifu 501-1193, Japan
[c] Department of Molecular Pathobiochemistry, Gifu University Graduate School of Medicine, Yanagido 1-1, Gifu 501-1193, Japan
[d] Department of Medical Technology, School of Health Sciences, Gifu University of Medical Science, Nagamine Ichihiraga 795-1, Seki, Gifu 501-3892, Japan
[e] Kazusa DNA Research Institute, Chiba 292-0818, Japan

ARTICLE INFO

Keywords:
ABL
G protein
NF-κB signaling
Rho
RhoGEF

ABSTRACT

The Rho family small GTPases mediate cell responses through actin cytoskeletal rearrangement. We previously reported that PLEKHG2, a Rho-specific guanine nucleotide exchange factor, is regulated via interaction with several proteins. We found that PLEKHG2 interacted with non-receptor tyrosine kinase ABL1, but the cellular function remains unclear. Here, we show that the interaction between PLEKHG2 and ABL1 attenuated the PLEKHG2-induced serum response element-dependent gene transcription in a tyrosine phosphorylation-independent manner. PLEKHG2 and ABL1 were co-localized and accumulated within cells co-expressing PLEKHG2 and ABL1. The cellular fractionation analysis suggested that the accumulation involved actin cytoskeletal reorganization. We also revealed that the co-expression of PLEKHG2 with ABL1, but not BCR-ABL, suppressed cell growth and synergistically enhanced NF-κB-dependent gene transcription. The cell growth suppression was canceled by co-expression with IκBα, a member of the NF-κB inhibitor protein family. This study suggests that the interaction between PLEKHG2 and ABL1 suppresses cell growth through intracellular protein accumulation via the NF-κB signaling pathway.

1. Introduction

Rho family small GTPases (Rho) regulate various cellular responses such as cell morphogenesis and proliferation through actin cytoskeletal rearrangement [1]. Rho acts as a binary switch cycling between an inactive GDP-bound state and an active GTP-bound state. Conversion to the GDP-bound state is mediated by intrinsic GTP hydrolysis, which can be stimulated by the actions of Rho-specific GTPase-activating proteins (RhoGAP). On the other hand, conversion to the GTP-bound state is promoted by the actions of Rho-specific guanine nucleotide exchange factors (RhoGEF), which facilitate the exchange of GDP for GTP on Rho [2]. A major subgroup of RhoGEF is the *diffuse B-cell lymphoma* (Dbl) family RhoGEF that contains a highly conserved Dbl homology (DH) domain, which catalyzes the GDP/GTP exchange, and is always arranged in tandem with a pleckstrin homology (PH) domain [3]. It is thought that RhoGEF is spatiotemporally regulated by various extracellular stimuli through membrane receptors during cell movement such as cell migration and invasion.

We previously reported that PLEKHG2, a Dbl family RhoGEF for Rac/Cdc42, was activated by interaction with heterotrimeric G protein Gβγ subunits, and enhanced the cell spreading [4]. On the other hand, we also recently reported that PLEKHG2 was negatively regulated by interaction with the heterotrimeric G protein Gαs subunit [5]. In addition, we reported that PLEKHG2 is regulated by certain binding molecules, such as β-actin and FHL1 [6–8]. In addition to being activated through extracellular stimulation via GPCR signaling and protein-protein interaction, PLEKHG2 is regulated by protein phosphorylation. We found that the regulation of PLEKHG2 via phosphorylation occurs through the epidermal growth factor receptor signaling pathway and EphB2/SRC signaling pathway [9,10]. In the latter pathway, Tyr489 of

Abbreviations: Rho, Rho family small GTPases; RhoGEF, Rho-specific guanine nucleotide exchange factor; Dbl, diffuse B-cell lymphoma; DH, Dbl homology; PH, pleckstrin homology; SH, src homology; FABD, F-actin binding domain; mAG, monomeric Azami Green; mKR, monomeric Keima Red; SRE, serum response element; NF-κB, nuclear factor-kappa B

* Corresponding author at: Department of Chemistry and Biomolecular Science, Faculty of Engineering, Gifu University, Yanagido1-1, Gifu 501-1193, Japan.
E-mail address: hueda@gifu-u.ac.jp (H. Ueda).

https://doi.org/10.1016/j.cellsig.2019.04.016
Received 27 December 2018; Received in revised form 31 March 2019; Accepted 1 April 2019
Available online 14 May 2019
0898-6568/

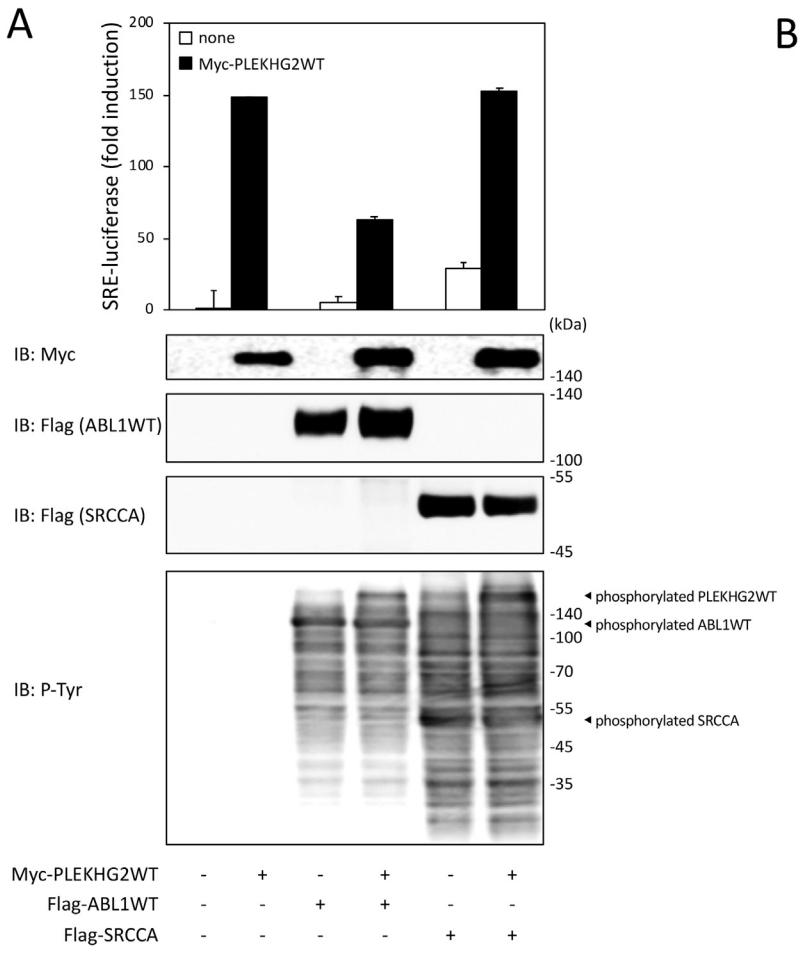

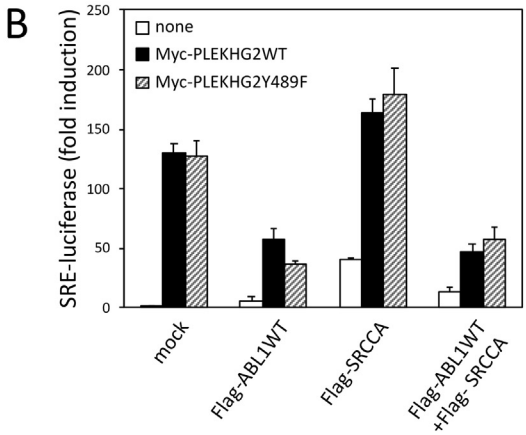

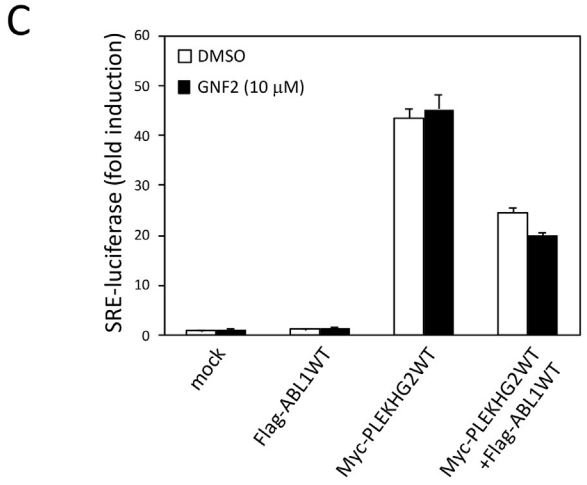

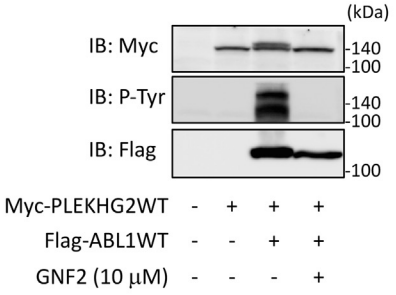

(caption on next page)

PLEKHG2 is phosphorylated by SRC in EPHB2-stimulated cells, and PLEKHG2 interacts with PIK3R3 and ABL1 through the recognition of phosphotyrosine 489 in PLEKHG2 via an Src homology (SH) 2 domain of PIK3R3 and ABL1. Moreover, it was confirmed that Tyr489 of PLEKHG2 is also phosphorylated by ABL1 as by SRC, and that PLEKHG2 interacted with ABL1 in a tyrosine phosphorylation-independent manner. However, the physiological functions of the interaction between PLEKHG2 and ABL1 remain unclear.

ABL1 is a non-receptor tyrosine kinase that belongs to ABL family kinases including ABL1/cAbl and ABL2/Arg [11]. Since there are several functional domains, including the SH2 domain, SH3 domain and F-actin binding domain (FABD), in the structure of ABL1, it is thought that ABL1 interacts with various molecules in the cell and regulates several biological processes involving Rho signaling-regulated actin

Fig. 1. Effects of ABL1 on PLEKHG2-induced SRE-dependent gene transcription.
(A) HEK293 cells were co-transfected with pSRE.L-luciferase, pRL-SV40, and expression vectors for Myc-PLEKHG2WT, Flag-ABL1WT and Flag-SRCCA, as indicated. Luciferase activities were determined with a dual-luciferase reporter assay system and normalized for transfection efficiency, and the relative activities are shown when the value of mock was taken as 1.0. The experiment was performed in triplicate, and the values are the means ± S.D. Cell lysates were immunoblotted with antibodies against Myc-epitope (for Myc-PLEKHG2WT) and phospho-tyrosine (for tyrosine-phosphorylated Myc-PLEKHG2WT). (B) HEK293 cells were co-transfected with pSRE.L-luciferase, pRL-SV40, and expression vectors for Myc-PLEKHG2WT and Myc-PLEKHG2Y489F, which is a Phe-substitution mutant of Tyr489, Flag-ABL1WT and/or Flag-SRCCA, as indicated. Luciferase activities were determined with a dual-luciferase reporter assay system and normalized for transfection efficiency, and the relative activities are shown when the value of mock was taken as 1.0. The experiment was performed in triplicate, and the values are the means ± S.D. (C) HEK293 cells were co-transfected with pSRE.L-luciferase, pRL-SV40, and expression vectors for Myc-PLEKHG2WT and Flag-ABL1WT, as indicated, and incubated in the absence or presence of 10 μM GNF2. Luciferase activities were determined with a dual-luciferase reporter assay system and normalized for transfection efficiency, and the relative activities are shown when the value of mock was taken as 1.0. The experiment was performed in triplicate, and the values are the means ± S.D. Cell lysates were immunoblotted with antibodies against Myc-epitope (for Myc-PLEKHG2WT), phospho-tyrosine (for tyrosine-phosphorylated Myc-PLEKHG2WT) and Flag-epitope (for Flag-ABL1WT). IB, immunoblotting.

cytoskeletal reorganization [12]. In axon patterning in Drosophila, ABL1 is known to modulate actin cytoskeletal rearrangement via Rac [13,14]. A previous study reported that ABL1 directly bound with the Rac-RhoGEF Trio via its SH3 domain in vitro [15]. In another report, ABL1 regulated a branched actin network in neurons by acting on Trio to stimulate Rac signaling in a tyrosine phosphorylation-dependent manner [16]. Further, another study reported that ABL1 activated and phosphorylated Sos-1, a dual guanine nucleotide exchange factor for Ras and Rac, in mammalian cells [17]. On the other hand, ABL1 contains three nuclear localization signal sequences and one nuclear export signal sequence, and it is thought that these amino acid sequences regulate the nucleus-cytoplasm localization of ABL1 [18]. A previous study reported that DNA damage by cisplatin induced ABL1 activation and the accumulation of p73, a p53-related gene product, to contribute to mismatch-repair-dependent apoptosis [19]. There is also a report that nuclear ABL1 directly interacts with the proline-rich region of the p73 protein via its SH3 domain and tyrosine-phosphorylates the p73 protein [20]. Therefore, ABL1 is related to cellular responses, but the mechanism by which ABL1 contributes to cell growth suppression is not completely understood.

In this study, we demonstrated that ABL1 attenuated PLEKHG2-induced serum response element (SRE)-dependent gene transcription in HEK293 cells via its interaction with PLEKHG2. We also observed that co-expression of PLEKHG2 and ABL1 caused the formation and accumulation of proteins containing PLEKHG2 and ABL1, and suppressed cell growth through the synergistic enhancement of the gene transcription dependent on nuclear factor-κB (NF-κB), which is known to be a critical regulator of cell growth. This is the first report to show that the interaction of RhoGEF with ABL1 causes the accumulation of intracellular proteins, which regulates cell growth through NF-κB signaling.

2. Materials and methods

2.1. Plasmids and reagents

The generation of pFN21A-Myc-PLEKHG2, pF5A-CMV-neoFlag-ABL1, and pF5A-CMV-neoFlag-SRCCA was described previously [9]. The various deletion mutants of PLEKHG2 or ABL1 were generated by PCR amplification and restriction enzyme digestion. To prepare glutathione S-transferase (GST)-fused proteins, ABL1 (515–949) and ABL1 (515–749) were subcloned into pGEX-4 T-1 vector by restriction enzyme digestion. pcDNA3.1-RacG12V and pcDNA3.1-Cdc42G12V were purchased from cDNA Resource Center. The RacG12V and Cdc42G12V were subcloned into pF5A-Flag vector by PCR amplification and restriction enzyme digestion. The pSRE.L-luciferase and pNF-κB.L-luciferase reporter plasmids were purchased from Stratagene, and pRL-SV40 was purchased from Nippon Gene. Monoclonal antibodies against cyclin E and cyclin B1 were purchased from Santa Cruz Biotechnology. Leptomycin B was purchased from Cayman Chemical.

2.2. Cell culture and transfection

HEK293 cells were grown in DMEM supplemented with 10% FBS at 37 °C. Transient transfection was performed using polyethylenimine (PolySciences Inc.). Cells were transfected with DNA for 6 h and then washed with serum-free DMEM or 10% FBS DMEM and incubated for 18 h.

2.3. Dual luciferase reporter gene assay

Cells seeded in 24-well plates were co-transfected with the indicated expression plasmids. After transfection, cells were washed once with ice-cold PBS and lysed with passive lysis buffer. Luciferase activities were determined by using a Dual-Luciferase Reporter assay system (Promega Co.). The activity of the experimental reporter was normalized against the activity of the control vector.

2.4. Immunoprecipitation

Transfected cells seeded in 6-cm dishes were washed once with ice-cold PBS and lysed with lysis buffer (50 mM Tris-HCl, pH 7.5, 100 mM NaCl, 0.1 mM EDTA, 1 mM Na_3VO_4, 0.5% Nonidet P-40, phosphatase inhibitor solution (Roche), and protease inhibitor solution (Roche)). The lysates were centrifuged to remove residue (16,100 xg for 10 min). Clear lysates were incubated with 1.0 μg of anti-Myc IgG for 2 h at 4 °C and then mixed with protein G-agarose beads (EMD Milipore Co.) for 1 h at 4 °C. The beads were washed three times with washing buffer (50 mM Tris-HCl, pH 7.5, 100 mM NaCl, 0.1 mM EDTA, 1 mM Na_3VO_4, 0.1% Nonidet P-40, phosphatase inhibitor solution, and protease inhibitor solution). Bound proteins were eluted with sample buffer and resolved by SDS-PAGE. The transferred PVDF membrane was blocked with PVDF Blocking Reagent for Can Get Signal (Toyobo Co.). For the detection of Myc-tag and Flag-tag, we used HRP-conjugated mouse anti-Myc IgG (FUJIFILM Wako Pure Chemical Co.) and mouse anti-Flag IgG (FUJIFILM Wako Pure Chemical Corp.), respectively. For the detection of P-Tyr and cABL, we used mouse anti-P-Tyr IgG (Santa Cruz) and anti-cABL (Santa Cruz). For the detection of these first antibody, we used HRP conjugated anti-mouse IgG (MBL Co.) and anti-rabbit IgG (MBL Co.) as secondary antibody. Visualization of HRP-labeled proteins was performed using enzyme-linked chemiluminescence (Thermo Fisher Scientific) and an LAS-4000 luminescent image analyzer (GE Healthcare).

2.5. In vitro binding assays

GST, GST-ABL1 (515–949) or GST-ABL1 (515–749) fusion proteins were expressed and extracted from *E. coli* strain BL21 and bound to glutathione-Sepharose 4B. Purified GST fusion protein (with the glutathione-agarose beads) and cell lysate were incubated for 2 h at 4 °C in lysis buffer. Beads were washed three times with lysis buffer, and bound proteins were separated by SDS-PAGE and detected by immunoblotting using various antibodies [9].

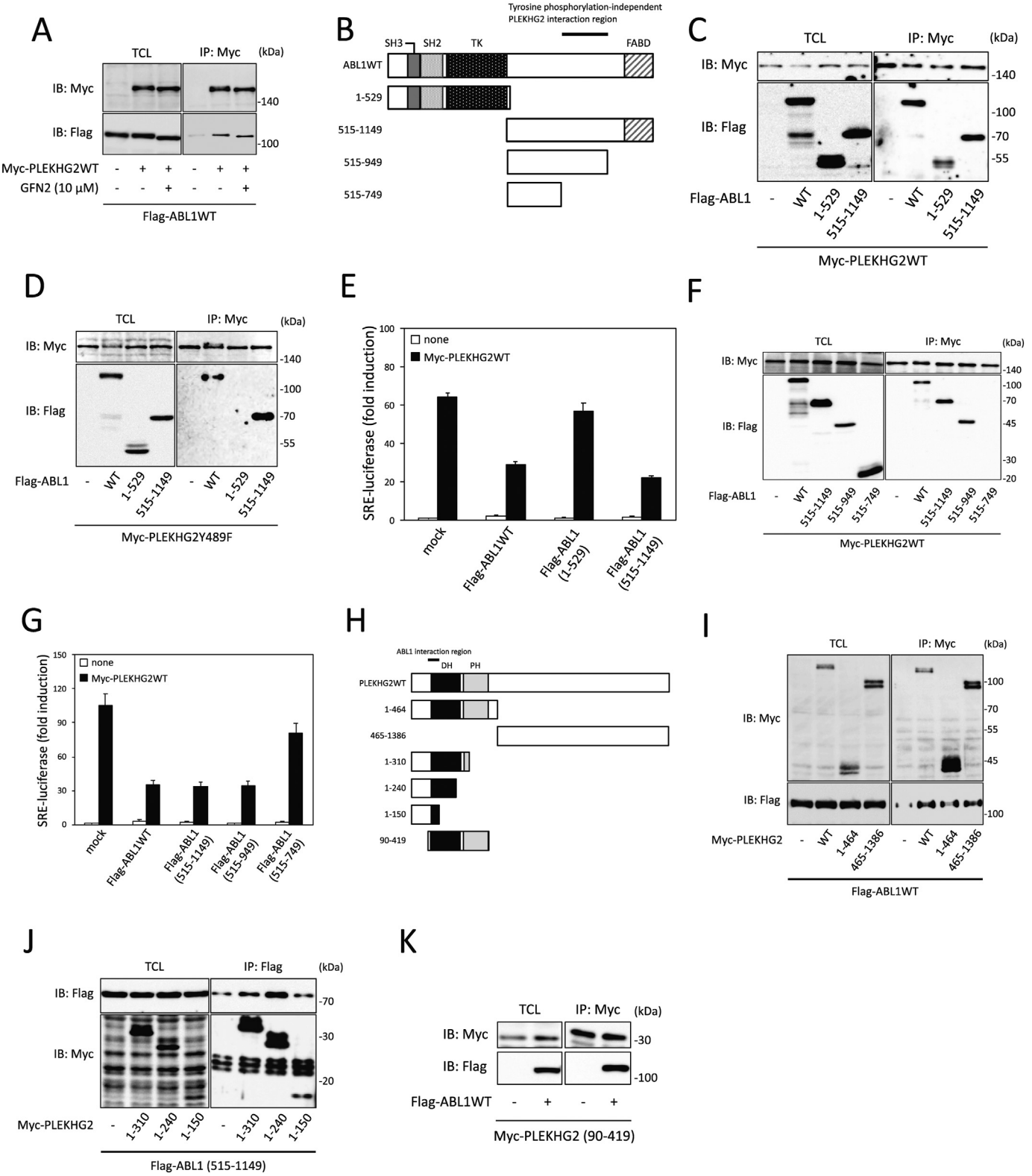

(caption on next page)

2.6. Immunofluorescent staining

Transfected cells cultured on cover slips were washed once with ice-cold PBS and fixed with 4% paraformaldehyde for 30 min. In the case of pretreatment by Triton X-100, transfected cells seeded onto glass were washed once with ice-cold PBS, detergent-extracted with lysis buffer (50 mM Tris-HCl, pH 7.5, 100 mM NaCl, 0.1 mM EDTA, 1 mM Na_3VO_4, 0.5% Triton X-100, phosphatase inhibitor solution and protease inhibitor solution) for 10 s and fixed with 4% paraformaldehyde for 30 min. Fixed cells were permeabilized with 0.1% Triton X-100 in PBS and washed four times with PBS. Then, cells were blocked with 10% goat serum in PBS for 1 h. Cells were washed with PBS and incubated

Fig. 2. Identification of the interaction regions between PLEKHG2 and ABL1, and effects of the various ABL1 mutants on PLEKHG2-induced SRE-dependent gene transcription.
(A) HEK293 cells were co-transfected with expression vectors for Myc-PLEKHG2WT and Flag-ABL1WT, as indicated, then incubated in the absence or presence of 10 μM GNF2. Cells were lysed 24 h after transfection, and immunoprecipitated with anti-Myc antibodies. Precipitated proteins were separated by SDS-PAGE and immunoblotted with anti-Myc antibody (for Myc-PLEKHG2WT) and anti-Flag antibody (for ABL1WT). TCL, total cell lysate; IP, immunoprecipitation; IB, immunoblotting (B) Structure of the proteins encoded by each expression plasmid: the WT, ABL1 (1–529), ABL1 (515–1149), ABL1 (515–949), and ABL1 (515–749) constructs code for amino acid residues 1–1149, 1–529, 515–1149, 515–949, and 515–749 of ABL1, respectively. We show the functional interacting region of PLEKHG2 (750–949). WT, wild type; SH2, Src homology 2 domain; SH3, Src homology 3 domain; TK, tyrosine kinase domain; FABD, F-actin binding domain; 1–529, ABL1 (1–529); 515–1149, ABL1 (515–1149); 515–949, ABL1 (515–949); 515–749, ABL1 (515–749) (C) HEK293 cells were co-transfected with expression vectors for Myc-PLEKHG2WT, Flag-ABL1WT, Flag-ABL1 (1–529) and Flag-ABL1 (515–1149), as indicated. Cells were lysed 24 h after transfection, and immunoprecipitated with anti-Myc antibodies. Precipitated proteins were separated by SDS-PAGE and immunoblotted with anti-Myc antibody (for Myc-PLEKHG2WT) and anti-Flag antibody (for ABL1WT and ABL1 mutants). WT, Flag-ABL1WT; 1–529, Flag-ABL1 (1–529); 515–1149, Flag-ABL1 (515–1149); TCL, total cell lysate; IP, immunoprecipitation; IB, immunoblotting (D) HEK293 cells were co-transfected with expression vectors for Myc-PLEKHG2Y489F, Flag-ABL1WT, Flag-ABL1 (1–529) and Flag-ABL1 (515–1149), as indicated. Cells were lysed 24 h after transfection, and immunoprecipitated with anti-Myc antibodies. Precipitated proteins were separated by SDS-PAGE and immunoblotted with anti-Myc antibody (for Myc-PLEKHG2Y489F) and anti-Flag antibody (for ABL1WT and ABL1 mutants). WT, Flag-ABL1WT; 1–529, Flag-ABL1 (1–529); 515–1149, Flag-ABL1 (515–1149); TCL, total cell lysate; IP, immunoprecipitation; IB, immunoblotting (E) HEK293 cells were co-transfected with pSRE.L-luciferase, pRL-SV40, and expression vectors for Myc-PLEKHG2WT, Flag-ABL1WT, Flag-ABL1 (1–529) and Flag-ABL1 (515–1149), as indicated. Luciferase activities were determined with a dual-luciferase reporter assay system and normalized for transfection efficiency, and the relative activities are shown when the value of mock was taken as 1.0. The experiment was performed in triplicate, and the values are the means ± S.D. (F) HEK293 cells were co-transfected with expression vectors for Myc-PLEKHG2WT, Flag-ABL1WT, Flag-ABL1 (515–1149), Flag-ABL1 (515–949) and Flag-ABL1 (515–749), as indicated. Cells were lysed 24 h after transfection, and immunoprecipitated with anti-Myc antibodies. Precipitated proteins were separated by SDS-PAGE and immunoblotted with anti-Myc antibody (for Myc-PLEKHG2WT) and anti-Flag antibody (for Flag-ABL1WT and Flag-ABL1 mutants). WT, Flag-ABL1WT; 515–1149, Flag-ABL1 (515–1149); 515–949, Flag-ABL1 (515–949); 515–749, Flag-ABL1 (515–749); TCL, total cell lysate; IP, immunoprecipitation; IB, immunoblotting (G) HEK293 cells were co-transfected with pSRE.L-luciferase, pRL-SV40, and expression vectors for Myc-PLEKHG2WT, Flag-ABL1WT, Flag-ABL1 (515–1149), Flag-ABL1 (515–949) and Flag-ABL1 (515–749), as indicated. Luciferase activities were determined with a dual-luciferase reporter assay system and normalized for transfection efficiency, and the relative activities are shown when the value of mock was taken as 1.0. The experiment was performed in triplicate, and the values are the means ± S.D. (H) Structure of the proteins encoded by each expression plasmid: the Myc-PLEKHG2WT, Myc-PLEKHG2 (1–464), Myc-PLEKHG2 (465–1386), Myc-PLEKHG2 (1–310), Myc-PLEKHG2 (1–240), Myc-PLEKHG2 (1–150) and Myc-PLEKHG2 (90–419) constructs code for amino acid residues 1–1386, 1–464, 465–1386, 1–310, 1–240, 1–150 and 90–419 of PLEKHG2, respectively. WT, Myc-PLEKHG2WT; DH, dbl. homology domain; PH, pleckstrin homology domain; 1–464, Myc-PLEKHG2 (1–464); 465–1386, Myc-PLEKHG2 (465–1386); 1–310, Myc-PLEKHG2 (1–310); 1–240, Myc-PLEKHG2 (1–240); 1–150, Myc-PLEKHG2 (1–150); 90–419, Myc-PLEKHG2 (90–419) (I) HEK293 cells were co-transfected with expression vectors for Flag-ABL1WT, Myc-PLEKHG2WT, Myc-PLEKHG2 (1–464) and Myc-PLEKHG2 (465–1386), as indicated. Cells were lysed 24 h after transfection, and immunoprecipitated with anti-Myc antibodies. Precipitated proteins were separated by SDS-PAGE and immunoblotted with anti-Myc antibody (for Myc-PLEKHG2WT and Myc-PLEKHG2 mutants) and anti-Flag antibody (for Flag-ABL1WT). WT, Myc-PLEKHG2WT; 1–464, Myc-PLEKHG2 (1–464); 465–1386, Myc-PLEKHG2 (465–1386); TCL, total cell lysate; IP, immunoprecipitation; IB, immunoblotting (J) HEK293 cells were co-transfected with expression vectors for ABL1WT, PLEKHG2WT, PLEKHG2 (1–310), PLEKHG2 (1–240) and PLEKHG2 (1–150), as indicated. Cells were lysed 24 h after transfection, and immunoprecipitated with anti-Myc antibodies. Precipitated proteins were separated by SDS-PAGE and immunoblotted with anti-Myc antibody (for Myc-PLEKHG2WT and Myc-PLEKHG2 mutants) and anti-Flag antibody (for Flag-ABL1WT). WT, Myc-PLEKHG2WT; 1–310, Myc-PLEKHG2 (1–310); 1–240, Myc-PLEKHG2 (1–240); 1–150, Myc-PLEKHG2 (1–150); TCL, total cell lysate; IP, immunoprecipitation; IB, immunoblotting (K) HEK293 cells were co-transfected with expression vectors for Flag-ABL1WT and Myc-PLEKHG2 (90–419), as indicated. Cells were lysed 24 h after transfection, and immunoprecipitated with anti-Myc antibodies. Precipitated proteins were separated by SDS-PAGE and immunoblotted with anti-Myc antibody (for Myc-PLEKHG2 (90–419)) and anti-Flag antibody (for Flag-ABL1WT). TCL, total cell lysate; IP, immunoprecipitation; IB, immunoblotting.

with the indicated primary antibodies and subsequently with secondary antibodies labeled with Alexa Fluor 488 (Life Technologies Co.) or Alexa Fluor 568 Phalloidin (Life Technologies Co.). The cover slips were then mounted with PermaFluor. Labeled cells were analyzed by a Zeiss laser scanning confocal microscope (LSM-710; Carl Zeiss).

2.7. Subcellular fractionation

Transfected cells seeded in 3-cm dishes were washed once with ice-cold PBS and lysed with lysis buffer (50 mM Tris-HCl, pH 7.5, 100 mM NaCl, 0.1 mM EDTA, 1 mM Na_3VO_4, 0.5% Triton X-100, phosphatase inhibitor solution, and protease inhibitor solution). The lysates were centrifuged to allow them to fractionate into clear lysates (Triton X-100 soluble) and residue (Triton X-100 insoluble) (16,100 xg for 10 min). Triton X-100 soluble and insoluble fractions were diluted with sample buffer. Detailed analysis of the subcellular localization of proteins was performed using a ProteoExtractTM Subcellular Proteome Extraction Kit (Merck). The subcellular fractionation was confirmed by immunoblotting using various antibodies against marker proteins (Cytoplasmic; Glyceraldehyde-3-phosphate dehydrogenase (GAPDH) form Proteintech, plasma membrane; Integrin β1 from BD Biosciences, Nuclear; Lamin from Cell Signaling Technology and Cytoskeletal; Vimentin from Sigma-Aldrich).

2.8. Cell-counting assay

Cells were co-transfected with the indicated expression plasmids. At 6 h after transfection, the cells were replated onto 24-well plates at a density of 2.0×10^4 cells per well. Cells were counted 1–3 days after replating.

2.9. Flow cytometric analysis of apoptosis

Cells were co-transfected with the indicated expression plasmids. At 24 h after transfection, cells were fixed and stained by using Tali Apoptosis Kit-Annexin V Alexa Fluor 488 (Thermo Fisher Scientific), and were analyzed by using cell analyzer EC800 (Sony Japan).

3. Results

3.1. ABL1 attenuated PLEKHG2 activity in a tyrosine phosphorylation-independent manner

To investigate whether ABL1 and SRC influence RhoGEF activity of PLEKHG2 in the cell, we measured the level of PLEKHG2-induced SRE-dependent gene transcription, which is known to be induced by Rho family activation [21]. The level of PLEKHG2-induced SRE-dependent gene transcription was attenuated in HEK293 cells co-expressing Myc-epitope-tagged wildtype PLEKHG2 (Myc-PLEKHG2WT) and Flag-epitope-tagged wildtype ABL1 (Flag-ABL1WT) as compared with cells

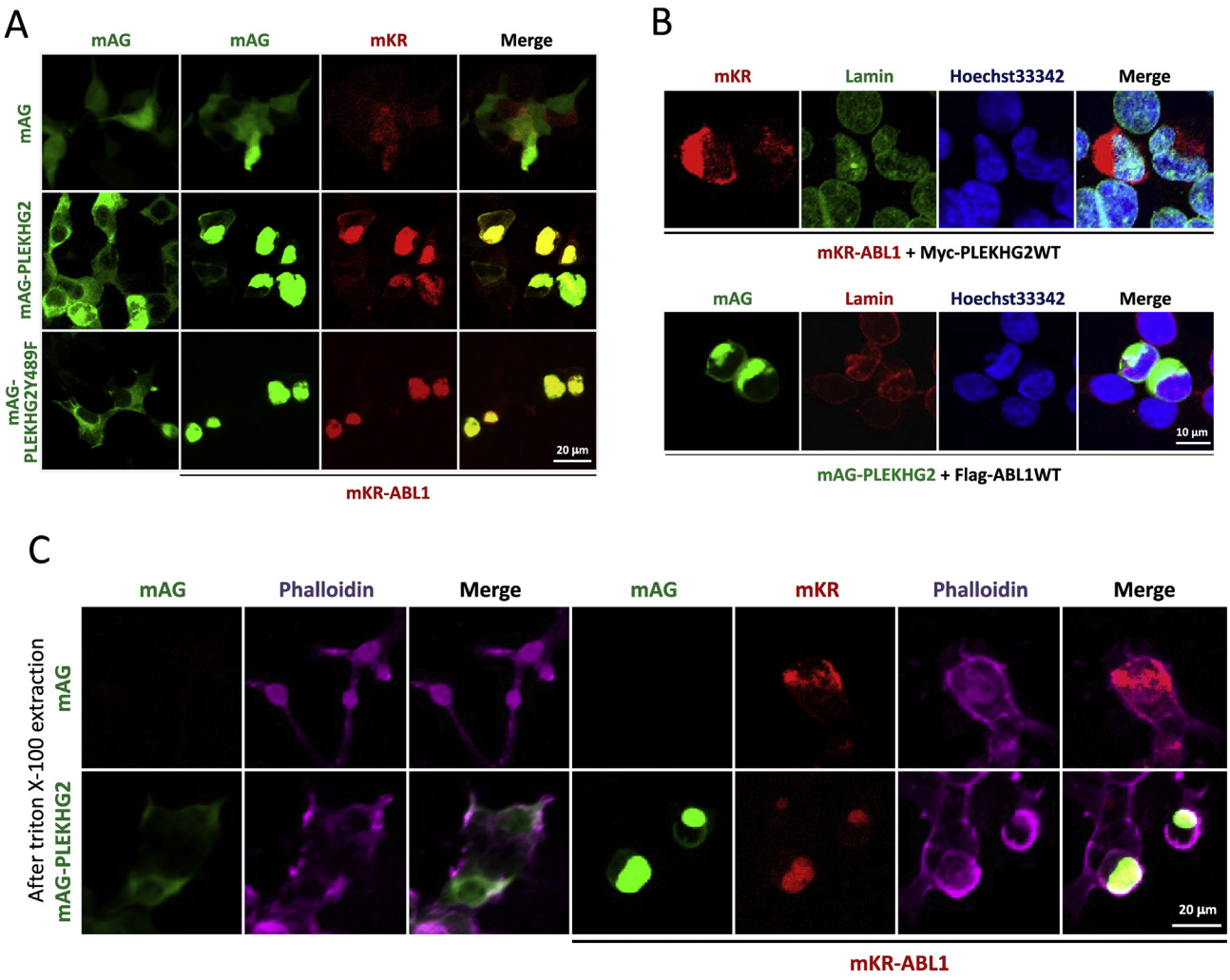

(caption on next page)

expressing Myc-PLEKHG2WT alone. On the other hand, the level of the SRE-dependent gene transcription did not change in cells co-expressing PLEKHG2WT and Flag-epitope-tagged constitutively active form of SRC (Flag-SRCCA) (Fig. 1A). We also observed that Myc-PLEKHG2WT was tyrosine-phosphorylated in cells co-expressing Myc-PLEKHG2WT and either Flag-ABL1WT or Flag-SRCCA (the over 140 kDa band is tyrosine-phosphorylated Myc-PLEKHG2WT, the 100 to 140 kDa band is tyrosine-phosphorylated Flag-ABL1WT and the 45 to 55 kDa band is tyrosine-phosphorylated Flag-SRCCA) (Fig. 1A). At this time, ABL1 suppressed PLEKHG2-induced SRE activation, however ABL1-resistant SRE activity

Fig. 3. Induction of intracellular protein accumulation in cells co-expressing PLEKHG2 and ABL1.
(A) HEK293 cells were co-transfected with mAG-tagged PLEKHG2WT (mAG-PLEKHG2), mAG-tagged PLEKHG2Y489F (mAG-PLEKHG2Y489F) and mKR-tagged ABL1WT (mKR-ABL1WT), as indicated. Transfected cells were fixed and observed by a confocal laser scanning microscope 24 h after transfection. mAG, monomeric Azami Green fluorescent protein; mKR, monomeric Keima Red fluorescent protein (B) HEK293 cells were co-transfected with mAG-PLEKHG2 and mKR-ABL1WT, as indicated. Transfected cells were fixed and were stained using an antibody against lamin and Hoechst 33342 and observed by a confocal laser scanning microscope. mAG, monomeric Azami Green fluorescent protein; mKR, monomeric Keima Red fluorescent protein (C) HEK293 cells were co-transfected with mAG, mAG-PLEKHG2 and mKR-ABL1WT, as indicated. Transfected cells were fixed after treatment with or without Triton X-100, then stained with Alexa568 conjugated Phalloidin and observed under a confocal laser scanning microscope. mAG, monomeric Azami Green fluorescent protein; mKR, monomeric Keima Red fluorescent protein (D) HEK293 cells were co-transfected with expression vectors for Flag-ABL1WT and Myc-PLEKHG2WT, as indicated. Transfected cells were fractionated using a subcellular fractionation kit. Fractionated proteins were separated by SDS-PAGE and immunoblotted with anti-Myc antibody (for Myc-PLEKHG2WT), anti-Flag antibody (for Flag-ABL1WT) and antibodies against each marker protein (Cytoplasmic; GAPDH, Plasma membrane; Integrin β1, Nuclear; Lamin and Cytoskeletal; Vimentin). IB, immunoblotting.

was still observed. Next, to examine whether ABL1 affects Rac1 and Cdc42-induced signaling activated by PLEKHG2, we measured the levels of SRE-dependent gene transcription in cells expressing Flag-epitope tagged constitutively active form of Rac1 (Flag-Rac1G12V) or Cdc42 (Flag-Cdc42G12V). As a result, the level of Flag-Rac1G12V-induced SRE-dependent gene transcription was attenuated in cells co-expressing Flag-Rac1G12V and Flag-ABL1WT as compared with cells expressing Flag-Rac1G12V alone. On the other hand, the level of Flag-Cdc42G12V-induced SRE-dependent gene transcription did not change in cells co-expressing Flag-Cdc42G12V and Flag-ABL1WT (Fig. S1). It was suggested that ABL1 acts not only on PLEKHG2 but also on Rac1 signaling, not on Cdc42 signaling. Next, to examine whether the tyrosine phosphorylation of PLEKHG2 by ABL1 is involved in the attenuation of PLEKHG2-induced SRE-dependent gene transcription, we measured the level of PLEKHG2-induced SRE-dependent gene transcription in cells co-expressing Flag-ABL1WT and Myc-epitope-tagged PLEKHG2 mutant containing a tyrosine-to-phenylalanine substitution at position 489 (Myc-PLEKHG2Y489F). As shown in Fig. 1B, the level of SRE-dependent gene transcription was attenuated in both cells co-expressing Flag-ABL1WT and either Myc-PLEKHG2WT or Myc-PLEKHG2Y489F. We did not find any significant difference between the attenuation of PLEKHG2WT-induced SRE-dependent gene transcription by ABL1WT and the attenuation of PLEKHG2Y489F-induced SRE-dependent gene transcription by ABL1WT. This result suggested that phosphorylation of Tyr489 at PLEKHG2 is not involved in the attenuation of PLEKHG2 activity by ABL1. Next, to examine whether ABL1 kinase activity is necessary for the attenuation of PLEKHG2 function by ABL1, we used GNF2, which is known to be an ABL1-specific kinase inhibitor. In the presence of GNF2, the level of PLEKHG2-induced SRE-dependent gene transcription was attenuated in the cells co-expressing Myc-PLEKHG2WT and Flag-ABL1WT. Under the same experimental condition, the tyrosine phosphorylation of Myc-PLEKHG2WT was inhibited in GNF2 treated cells co-expressing Myc-PLEKHG2WT and Flag-ABL1WT (Fig. 1C). These results suggested that ABL1 attenuates PLEKHG2 function in a tyrosine phosphorylation-independent manner.

3.2. The PLEKHG2 activity attenuation was related to the interaction between PLEKHG2 and ABL1

Since the tyrosine phosphorylation of PLEKHG2 by ABL1 can be considered to be less involved in the attenuation of PLEKHG2 activity by ABL1, we examined the previous reported tyrosine phosphorylation-independent interaction between PLEKHG2 and ABL1 [9]. First, to confirm the tyrosine phosphorylation-independent interaction of PLEKHG2 with ABL1, Myc-PLEKHG2WT was immunoprecipitated with a specific antibody against the Myc-epitope in GNF2-treated cells co-expressing Myc-PLEKHG2WT and Flag-ABL1WT. As a result, Flag-ABL1WT was co-immunoprecipitated with Myc-PLEKHG2WT regardless of whether GNF2 was present (Fig. 2A). This result suggested that ABL1 interacts with PLEKHG2 in a tyrosine phosphorylation-independent manner, as we reported previously [9]. To investigate whether the region of ABL1 interacts with PLEKHG2, several Flag-epitope-tagged truncated mutants of ABL1 were prepared as in Fig. 2B. An immunoprecipitation experiment was performed, and showed that both Flag-ABL1 (1–529) and Flag-ABL1 (515–1149) were co-precipitated with Myc-PLEKHG2WT (Fig. 2C), but only Flag-ABL1 (515–1149) was co-precipitated with Myc-PLEKHG2Y489F (Fig. 2D). In addition, Flag-SRCCA was also co-precipitated with Myc-PLEKHG2WT (Fig. S2A). This result suggests that the SH2 of ABL1 interacts with phosphorylated Tyr489 of PLEKHG2. Next, we examined whether these mutants of ABL1 influence the attenuation of PLEKHG2 activity. The results of this experiment showed that the level of PLEKHG2-induced SRE-dependent gene transcription was attenuated in cells co-expressing Myc-PLEKHG2WT and Flag-ABL1 (515–1149), whereas there was almost no attenuation of the PLEKHG2-induced SRE-dependent gene transcription level in cells co-expressing Myc-PLEKHG2WT and Flag-ABL1 (1–529) (Fig. 2E). These findings suggested that certain amino acid sequences are indispensable for the attenuation of PLEKHG2 activity in the 515–1149 amino acid sequences of ABL1. To elucidate the PLEKHG2 interaction region of ABL1 in detail, we performed an immunoprecipitation experiment using several truncated mutants of ABL1 as shown in Fig. 2B. As a result, Flag-ABL1 (515–949) was co-precipitated with Myc-PLEKHG2WT, but Flag-ABL1 (515–749) was not (Fig. 2F). We also examined the effect of these mutants on the level of the PLEKHG2-induced SRE-dependent gene transcription. The level of PLEKHG2-induced SRE-dependent gene transcription was attenuated in cells co-expressing Myc-PLEKHG2WT and Flag-ABL1 (515–949), but the degree of its attenuation was very low in cells co-expressing Myc-PLEKHG2WT and Flag-ABL1 (515–749) (Fig. 2G). These results suggest that the region of amino acids 750 to 949 in ABL1 is important for the interaction with PLEKHG2 and the attenuation of PLEKHG2 RhoGEF activity (marked by the bar in Fig. 2B).

Next, to investigate whether the region of PLEKHG2 interacts with ABL1, several Myc epitope-tagged truncated mutants of PLEKHG2 were prepared as in Fig. 2H, and we performed an immunoprecipitation experiment using these mutants. As shown in Fig. 2I, Flag-ABL1WT was co-precipitated with both Myc-PLEKHG2 (1–464) and Myc-PLEKHG2 (465–1386). The region of amino acids 1–464 in PLEKHG2 contains a DH domain and PH domain, both of which are important for the RhoGEF activity of PLEKHG2. We therefore focused on the region of amino acids 1–464 in PLEKHG2. Next, to examine which region of PLEKHG2 interacted with ABL1, we performed the immunoprecipitation experiment using Flag-ABL1 (515–1149) containing a PLEKHG2-interaction region. This experiment showed that Myc-PLEKHG2 (1 − 310), Myc-PLEKHG2 (1–240) and Myc-PLEKHG2 (1–150) were co-precipitated with Flag-ABL1 (515–1149) (Fig. 2J). Moreover, Flag-ABL1WT was co-precipitated with Myc-PLEKHG2 (90–419) (Fig. 2K). These results suggested that the region of amino acids 90 to 150 in PLEKHG2 is important for the interaction with ABL1 (marked by the bar in Fig. 2H). Next, to examine whether ABL1 directly interacts with PLEKHG2, Myc-PLEKHG2-expressing cells lysates and Flag-ABL1-expressing cells lysates were respectively prepared, and the immunoprecipitation experiment was performed using the lysates which mixed them. As a result, co-immunoprecipitation of Flag-ABL1WT with Myc-PLEKHG2WT was not detected (Fig. S2B). Next, to examine

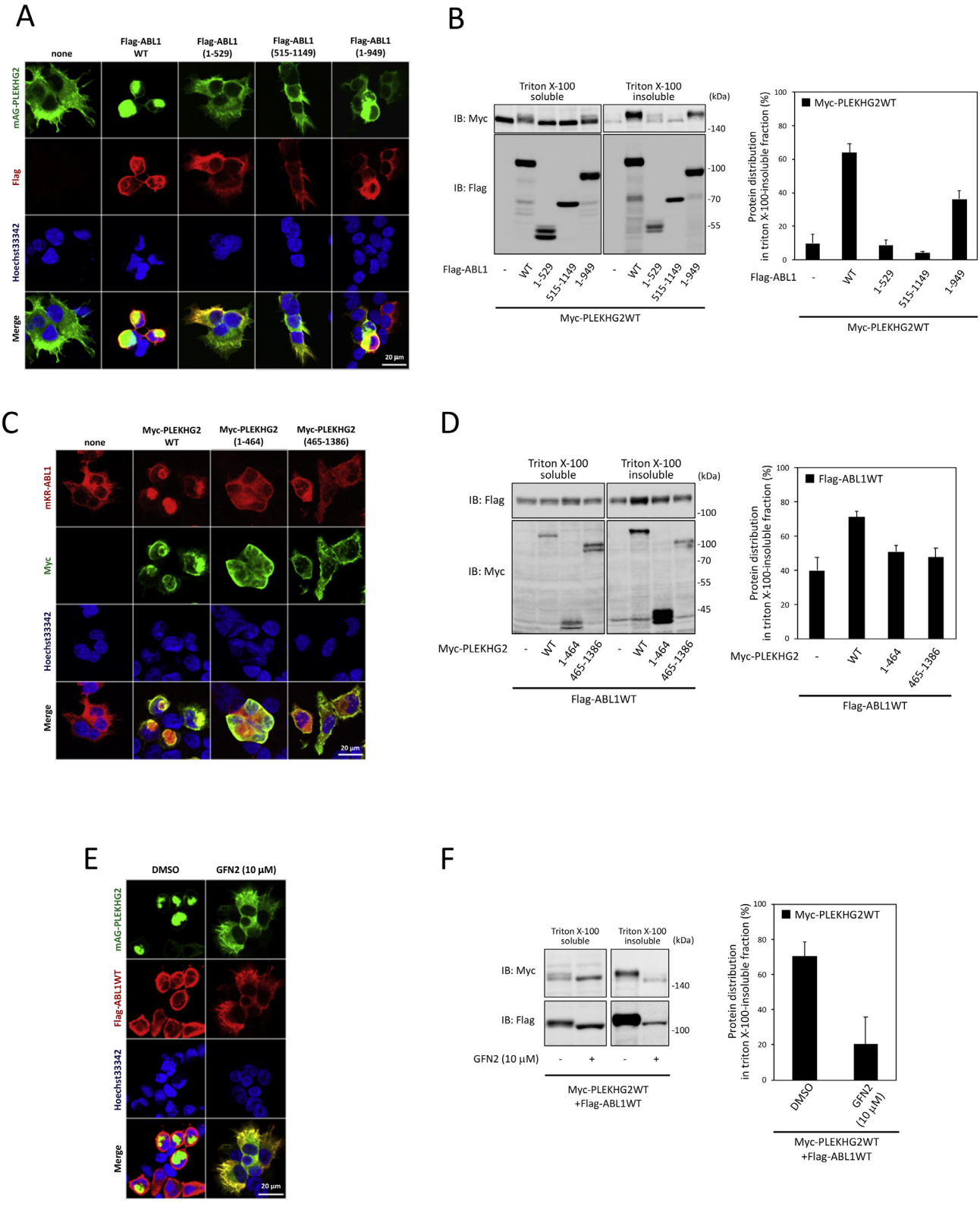

(caption on next page)

whether ABL1 directly binds to PLEKHG2, we analyzed the binding using a GST pull-down assay. GST, GST-fused ABL1 (515–949) (GST-ABL1 (515–949)) and GST-fused ABL1 (515–749) (GST-ABL1 (515–749)) were expressed in *E. coli* and purified on glutathione-Sepharose beads. We performed pull-down assays from Myc-PLEKHG2WT-expressing cells lysates using GST, GST-ABL1 (515–949) or GST-ABL1 (515–749) bound to glutathione-Sepharose beads. As a result, co-precipitation of each GST protein with Myc-PLEKHG2WT was not detected (Fig. S2C). Furthermore, we performed pull-down assays from Myc-PLEKHG2 (90–419)-expressing cells lysates using GST, GST-ABL1 (515–949) or GST-ABL1 (515–749) bound to glutathione-Sepharose beads. As a result, co-precipitation of Myc-PLEKHG2 (90–419)

Fig. 4. Both tyrosine phosphorylation-dependent and -independent involvement of ABL1 were required for the intracellular accumulation of PLEKHG2 and ABL1. (A) HEK293 cells were co-transfected with expression vectors for mAG-PLEKHG2WT, Flag-ABL1WT, Flag-ABL1 (1–529), Flag-ABL1 (515–1149) and Flag-ABL1 (1–949), as indicated. Transfected cells were fixed and observed under a confocal laser scanning microscope. (B) HEK293 cells were co-transfected with expression vectors for Myc-PLEKHG2WT, Flag-ABL1WT, Flag-ABL1 (1–529), Flag-ABL1 (515–1149) and Flag-ABL1 (1–949), as indicated. Transfected cells were fractionated into Triton X-100-soluble and -insoluble fractions. Fractionated proteins were separated by SDS-PAGE and immunoblotted with anti-Myc antibody (for Myc-PLEKHG2WT) and anti-Flag antibody (for Flag-ABL1WT and Flag-ABL1 mutants). The rate of band intensity of Myc-PLEKHG2WT, (Triton X-100 insoluble)/(Triton X-100 soluble + insoluble) (%), was quantitated as indicated. The data shown are representative of three independent experiments, and the values are the means ± S.D. IB, immunoblotting; WT, Flag-ABL1WT; 1–529, Flag-ABL1 (1–529); 515–1149, Flag-ABL1 (515–1149); 1–949, Flag-ABL1 (1–949) (C) HEK293 cells were co-transfected with expression vectors for mKR-ABL1WT, Myc-PLEKHG2WT, Myc-PLEKHG2 (1–464) and Myc-PLEKHG2 (465–1386), as indicated. Transfected cells were fixed and observed under a confocal laser scanning microscope. (D) HEK293 cells were co-transfected with expression vectors for Flag-ABL1WT, Myc-PLEKHG2WT, Myc-PLEKHG2 (1–464) and Myc-PLEKHG2 (465–1386), as indicated. Transfected cells were fractionated into Triton X-100-soluble and -insoluble fractions. Fractionated proteins were separated by SDS-PAGE and immunoblotted with anti-Myc antibody (for Myc-PLEKHG2WT and Myc-PLEKHG2 mutants) and anti-Flag antibody (for Flag-ABL1WT). The rate of band intensity of Flag-ABL1WT, (Triton X-100 insoluble)/(Triton X-100 soluble + insoluble) (%), was quantitated as indicated. The data shown are representative of three independent experiments, and the values are the means ± S.D. IB, immunoblotting; WT, PLEKHG2WT; 1–464, PLEKHG2 (1–464); 465–1386, PLEKHG2 (465–1386) (E) HEK293 cells were co-transfected with expression vectors for Flag-ABL1WT and mAG-PLEKHG2, as indicated, then incubated in the absence or presence of 10 μM GNF2. Transfected cells were fixed and observed under a confocal laser scanning microscope. DMSO, dimethyl sulfoxide (F) HEK293 cells were co-transfected with expression vectors for Flag-ABL1WT and Myc-PLEKHG2WT, as indicated, then incubated in the absence or presence of 10 μM GNF2. Transfected cells were fractionated into Triton X-100-soluble and -insoluble fractions. Fractionated proteins were separated by SDS-PAGE and immunoblotted with anti-Myc antibody (for Myc-PLEKHG2WT) and anti-Flag antibody (for Flag-ABL1WT). The rate of band intensity of Myc-PLEKHG2WT, (Triton X-100 insoluble)/(Triton X-100 soluble + insoluble) (%), was quantitated as indicated. The data shown are representative of three independent experiments, and the values are the means ± S.D. IB, immunoblotting.

with GST-ABL1 (515–949) was detected, but not with GST and GST-ABL1 (515–749) (Fig. S2D). From these results, it is considered that amino acids 750 to 949 in ABL1 and amino acids 90 to 150 in PLEKHG2 can directly interact. However, since co-precipitation with Myc-PLEKHG2WT was not detected, it is thought that some structural change containing phosphorylation and interaction with other proteins in PLEKHG2 and/or ABL1 is required in cells.

3.3. Interaction of PLEKHG2 with ABL1 induced intracellular protein accumulation

Next, to examine how the interaction of PLEKHG2 and ABL1 influences the intracellular localization of these proteins and the cell morphology, we performed immunostaining using several antibodies and images of cells were obtained using a confocal laser scanning microscope with monomeric Azami-Green (mAG) and monomeric Keima-Red (mKR). Analysis of the fluorescence of mAG revealed that PLEKHG2 was diffusely distributed in the cytoplasm and near the plasma membranes in cells expressing mAG fused to the N-terminal of PLEKHG2 (mAG-PLEKHG2). On the other hand, PLEKHG2 was strongly accumulated near the center of the cell in cells co-expressing mAG-PLEKHG2 and mKR fused to the N-terminal of ABL1 (mKR-ABL1). At the same time, the observation of mKR fluorescence demonstrated that ABL1 was co-localized with PLEKHG2 (Fig. 3A). Moreover, PLEKHG2Y489F was also co-localized with ABL1 in the cells co-expressing mAG-PLEKHG2Y489F and mKR-ABL1. These results suggest that the interaction of PLEKHG2 with ABL1 causes the accumulation of intracellular proteins in a tyrosine phosphorylation-independent manner. Next, to investigate whether the accumulation of PLEKHG2 and ABL1 observed near the center of this cell was localized in the nucleus, we performed immunostaining for lamin, a marker of the nuclear envelope. The results showed that neither PLEKHG2 nor ABL1 was co-localized with lamin (Fig. 3B). We also observed the localization of PLEKHG2 and ABL1 by using leptomycin B. In this situation, PLEKHG2 and ABL1 were co-localized in cytoplasm (data not shown). These in turn suggested that the accumulation of PLEKHG2 and ABL1 was localized in cytoplasm. Previously, we reported that PLEKHG2 is an actin-binding protein [6]. It is also known that ABL1 contains FABD and is localized to the filamentous actin cytoskeleton [22]. Based on these earlier observations, we considered that the accumulation of PLEKHG2 and ABL1 might be localized to the filamentous actin cytoskeleton. To examine this possibility, cell proteins were extracted with Triton X-100 before paraformaldehyde fixation, since F-actin binding protein is known to exhibit resistance to Triton X-100 extraction [23]. As a result, the fluorescence of mAG disappeared by treatment with Triton X-100 in cells co-expressing mAG and mKR-ABL1, although the fluorescence of mKR remained. On the other hand, the fluorescence of both mAG and mKR was resistant to Triton X-100 treatment in cells co-expressing mAG-PLEKHG2 and mKR-ABL1 (Fig. 3C). These results suggest that PLEKHG2 and ABL1, which show co-localization and intracellular accumulation, interact with F-actin. In addition, to confirm the subcellular localization of PLEKHG2 and ABL1, we performed subcellular fractionation analysis. As a result, it was revealed that the distribution of PLEKHG2 to the Vimentin-rich cytoskeletal fraction was significantly increased in cells co-expressing Myc-PLEKHG2WT and Flag-ABL1WT, compared with cells expressing Myc-PLEKHG2WT alone (Fig. 3D). These results suggested that the intracellular accumulation of PLEKHG2 and ABL1 may be related to the interaction of F-actin with PLEKHG2 or ABL1 or both.

3.4. Both tyrosine phosphorylation-dependent and -independent involvement of ABL1 were required for the intracellular accumulation of PLEKHG2 and ABL1

Next, to examine which structures of ABL1 and PLEKHG2 are required for the intracellular protein accumulation, we used cells expressing various mutants of ABL1 and PLEKHG2, respectively. First, to examine which structures of ABL1 are required for the intracellular protein accumulation, we investigated the subcellular localization of PLEKHG2 in cells co-expressing mAG-PLEKHG2 and three ABL1 mutants. We found that the accumulation was induced in cells co-expressing mAG-PLEKHG2 and Flag-ABL1WT, but not Flag-ABL1 (1–529) and Flag-ABL1 (515–1149). In cells co-expressing mAG-PLEKHG2 and Flag-ABL1 (1–949), a truncated mutant deficient in FABD of ABL1, the accumulation was observed, but to a much lesser degree than in cells co-expressing mAG-PLEKHG2 and Flag-ABL1WT (Fig. 4A). Myc-PLEKHG2WT was also distributed in the Triton X-100 insoluble fraction in cells co-expressing Myc-PLEKHG2WT with Flag-ABL1WT, although there was no Myc-PLEKHG2WT distribution in the Triton X-100 insoluble fraction in cells lacking the protein accumulation, which co-expressed Flag-ABL1 (1–529) and Flag-ABL1 (515–1149). On the other hand, PLEKHG2 was distributed in the Triton X-100 insoluble fraction in cells co-expressing Myc-PLEKHG2WT with Flag-ABL1 (1–949), which was similar to the finding in cells co-expressing Myc-PLEKHG2WT with Flag-ABL1WT, which exhibited the protein accumulation (Fig. 4B). From the results of immunoblotting of Vimentin and GAPDH, it was confirmed that the cell fractionation with Triton X-100 was correctly performed. (Fig. S3) These results suggested that the PLEKHG2 interaction region and the region containing the kinase, SH2 and SH3 domains of ABL1 are required for induction of intracellular

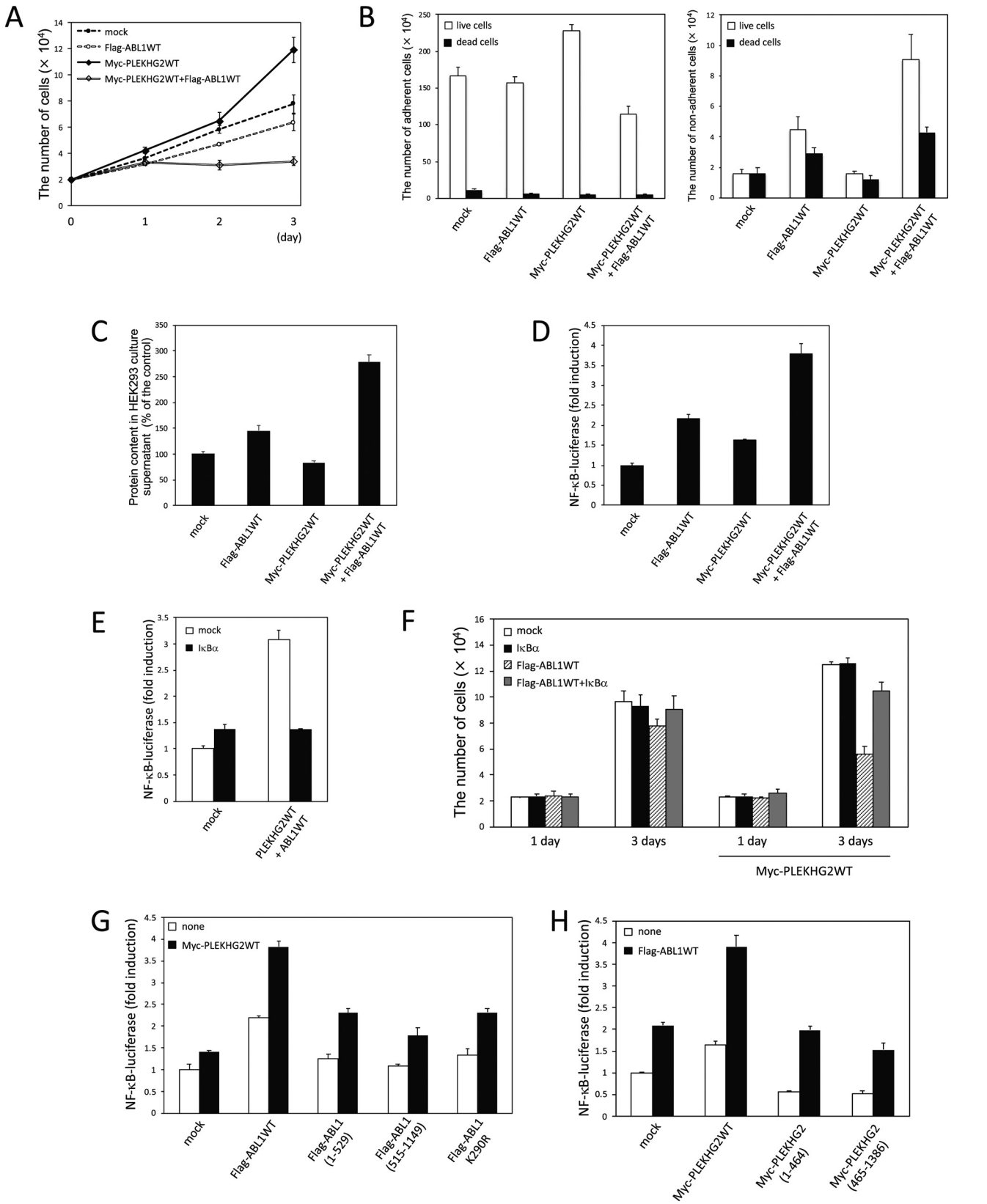

(caption on next page)

accumulation by PLEKHG2 and ABL1. To examine which structures of PLEKHG2 are required for the intracellular protein accumulation, we investigated the subcellular localization of ABL1 in cells co-expressing mKR-ABL1 and two PLEKHG2 mutants, respectively. The results showed that the accumulation was only induced in cells co-expressing mKR-ABL1 and Myc-PLEKHG2WT, and not in those co-expressing Myc-PLEKHG2 (1–464) and Myc-PLEKHG2 (465–1386) (Fig. 4C). Similarly, Flag-ABL1WT was only distributed in the Triton X-100 insoluble

Fig. 5. Intracellular protein accumulation suppressed the cell growth through the NF-κB signaling pathway.
(A) HEK293 cells were co-transfected with expression vectors for Flag-ABL1WT and Myc-PLEKHG2WT, as indicated. The number of tranfected cells was counted daily from 1 to 3 days after replating. The data shown are representative of three independent experiments, and the values are the means ± S.D. (B) HEK293 cells were co-transfected with expression vectors for Flag-ABL1WT and Myc-PLEKHG2WT, as indicated. At 6 h after transfection, the cells were replated onto 6-cm dishes at a density of 5.0×10^5 cells. The number of adhesion or floating cells was counted after resuspension with trypan blue at 3 days. The data shown are representative of three independent experiments, and the values are the means ± S.D. (C) HEK293 cells were co-transfected with expression vectors for Flag-ABL1WT and Myc-PLEKHG2WT, as indicated. Protein contents in the culture supernatant from the transfected cells were measured by BCA assay. The data shown are representative of three independent experiments, and the values are the means ± S.D. (D) HEK293 cells were co-transfected with pNF-κB-luciferase, pRL-SV40, and expression vectors for Myc-PLEKHG2WT and Flag-ABL1WT, as indicated. Luciferase activities were determined with a dual-luciferase reporter assay system and normalized for transfection efficiency, and the relative activities are shown when the value of mock was taken as 1.0. The experiment was performed in triplicate, and the values are the means ± S.D. (E) HEK293 cells were co-transfected with pNF-κB-luciferase, pRL-SV40, and expression vectors for Myc-PLEKHG2WT, Flag-ABL1WT and IκBα, as indicated. Luciferase activities were determined with a dual-luciferase reporter assay system and normalized for transfection efficiency, and the relative activities are shown when the value of mock was taken as 1.0. The experiment was performed in triplicate, and the values are the means ± S.D. (F) HEK293 cells were co-transfected with expression vectors for Flag-ABL1WT, Myc-PLEKHG2WT, and IκBα, as indicated. The number of transfected cells was counted at 1 and 3 days after replating. The data shown are representative of three independent experiments, and the values are the means ± S.D. (G) HEK293 cells were co-transfected with pNF-κB-luciferase, pRL-SV40, and expression vectors for Myc-PLEKHG2WT, Flag-ABL1WT, Flag-ABL1 (1–529), Flag-ABL1 (515–1149) and ABL1K290R, as indicated. Luciferase activities were determined with a dual-luciferase reporter assay system and normalized for transfection efficiency, and the relative activities are shown when the value of mock was taken as 1.0. The experiment was performed in triplicate, and the values are the means ± S.D. (H) HEK293 cells were co-transfected with pNF-κB-luciferase, pRL-SV40, and expression vectors for Flag-ABL1WT, Myc-PLEKHG2WT, Myc-PLEKHG2 (1–464), and Myc-PLEKHG2 (465–1386), as indicated. Luciferase activities were determined with a dual-luciferase reporter assay system and normalized for transfection efficiency, and the relative activities are shown when the value of mock was taken as 1.0. The experiment was performed in triplicate, and the values are the means ± S.D.

fraction in cells co-expressing Flag-ABL1WT with Myc-PLEKHG2WT, and not in those co-expressing Myc-PLEKHG2 (1–464) and Myc-PLEKHG2 (465–1386) (Fig. 4D). These results suggested that the whole structure of PLEKHG2 is required for induction of intracellular protein accumulation by PLEKHG2 and ABL1. Next, to examine whether the tyrosine kinase activity of ABL1, which is not necessary for the interaction of PLEKHG2 with ABL1, is necessary for the induction of intracellular protein accumulation, cells co-expressing mAG-PLEKHG2WT and Flag-ABL1WT were treated with GNF2. As a result, the intracellular protein accumulation disappeared in GNF2-treated cells co-expressing mAG-PLEKHG2 and Flag-ABL1WT (Fig. 4E). At the same time, the amount of Myc-PLEKHG2 distributed in the Triton X-100 insoluble fraction decreased (Fig. 4F). However, since mAG-PLEKHG2Y489F has the ability to induce intracellular accumulation (Fig. 3A), it seems possible that the phosphorylation of another protein by ABL1 is necessary to induce the accumulation. Further research on this point will be needed in the future.

3.5. Intracellular protein accumulation suppressed cell growth through the NF-κB signaling pathway

To identify the physiological roles of the intracellular protein accumulation, we examined the effect of this accumulation on cell proliferation. The growth rate of the cells co-expressing Myc-PLEKHG2WT and Flag-ABL1WT was slower than that of the other cells (Fig. 5A). Additionally, we evaluated the number of mAG-positive cells co-expressing Myc-PLEKHG2WT and/or Flag-ABL1WT, and curtained the growth rate of the cells co-expressing Myc-PLEKHG2WT and Flag-ABL1WT was slower than that of the other cells, just as Fig. 5A and Supply Fig. S4A. We also found that the number of both live and dead floating cells among the cells co-expressing Myc-PLEKHG2WT and Flag-ABL1WT was increased, compared to the number of floating cells among the other cells (Fig. 5B). Therefore, to quantify the number of floating cells, we measured the amount of protein in the cells from the culture supernatant. The results showed that the amount of protein in cells co-expressing Myc-PLEKHG2WT and Flag-ABL1WT was higher than the protein amounts in the other cells (Fig. 5C). This suggested that cell death, the inhibition of cell adhesion and/or cell growth arrest is induced in cells co-expressing Myc-PLEKHG2WT and Flag-ABL1WT. Next, we tried to examine the involvement of cell death and cell cycle arrest. First, to examine whether apoptosis is involved in this decrease in cell growth rate, we performed Annexin V-fluorescein isothiocyanate (FITC)/propidium iodide (PI) staining on cells co-expressing Myc-PLEKHG2WT and/or Flag-ABL1WT. As a result, cells co-expressing Myc-PLEKHG2WT and Flag-ABL1WT increased the number of Annexin V-FITC- and PI-positive cells considered to be dead cells as compared to the mock cells, but not Annexin V-positive cells considered to be early apoptotic cells (Fig. S4B). Furthermore, to examine whether cell cycle arrest is involved in this decrease in cell growth rate, we analyzed the amount of cyclin E and cyclin B1 by immunoblotting. As a result, neither quantitative change of cyclin E nor cyclin B1 was observed in each cell (Fig. S4C). From these results, detail mechanisms of apoptosis and growth arrest in cells co-expressing PLEKHG2WT and ABL1WT have not been clarified. Further investigations will be needed.

In general, it is well-known that NF-κB signaling plays important roles in cell survival or cell death [24–26]. To examine whether NF-κB signaling is involved in the cell growth suppression in cells co-expressing Myc-PLEKHG2WT and Flag-ABL1WT, we measured the level of the NF-κB-dependent gene transcription. We found that the level of NF-κB-dependent gene transcription was synergistically enhanced in cells co-expressing Myc-PLEKHG2WT and Flag-ABL1WT as compared with that in cells expressing either Myc-PLEKHG2WT or Flag-ABL1WT alone (Fig. 5D). These results suggest that NF-κB signaling is related to cell growth suppression in cells co-expressing Myc-PLEKHG2WT and Flag-ABL1WT. Next, to examine how the NF-κB signaling pathway is related to the cell growth suppression, we studied cell growth using an inhibitor of NF-κB (IκBα). First, it was confirmed that IκBα suppressed the enhancement of the level of NF-κB-dependent gene transcription in the cells co-expressing Myc-PLEKHG2WT and Flag-ABL1WT (Fig. 5E). Next, we examined whether IκBα affects cell growth suppression in cells co-expressing Myc-PLEKHG2WT and Flag-ABL1WT. This experiment showed that cell proliferation was significantly restored in cells co-expressing IκBα, in contrast to the cell growth suppression observed in cells co-expressing Myc-PLEKHG2WT and Flag-ABL1WT (Fig. 5F). These results suggested that the cell growth suppression was regulated through the NF-κB signaling pathway in cells co-expressing Myc-PLEKHG2WT and Flag-ABL1WT. To investigate which structures of ABL1 and PLEKHG2 are involved in the enhancement of the NF-κB signaling pathway in cells co-expressing PLEKHG2 and ABL1, we measured the level of the NF-κB-dependent gene transcription using various mutants of ABL1 and PLEKHG2. We found that the level of the NF-κB-dependent gene transcription in cells co-expressing Myc-PLEKHG2WT and either Flag-ABL1 (1–529) or Flag-ABL1 (515–1149) was lower than the transcriptional activity level in cells co-expressing Flag-ABL1WT and Myc-PLEKHG2WT. Similarly, the level of the NF-κB-dependent gene transcription in cells co-expressing Myc-PLEKHG2WT and Flag-ABL1 K290R, a kinase-dead mutant, was also lower than the transcriptional activity level in cells co-expressing Flag-ABL1WT and Myc-PLEKHG2WT (Fig. 5G). On the other hand, the level of the NF-κB-dependent gene transcription in cells co-expressing Flag-ABL1WT and

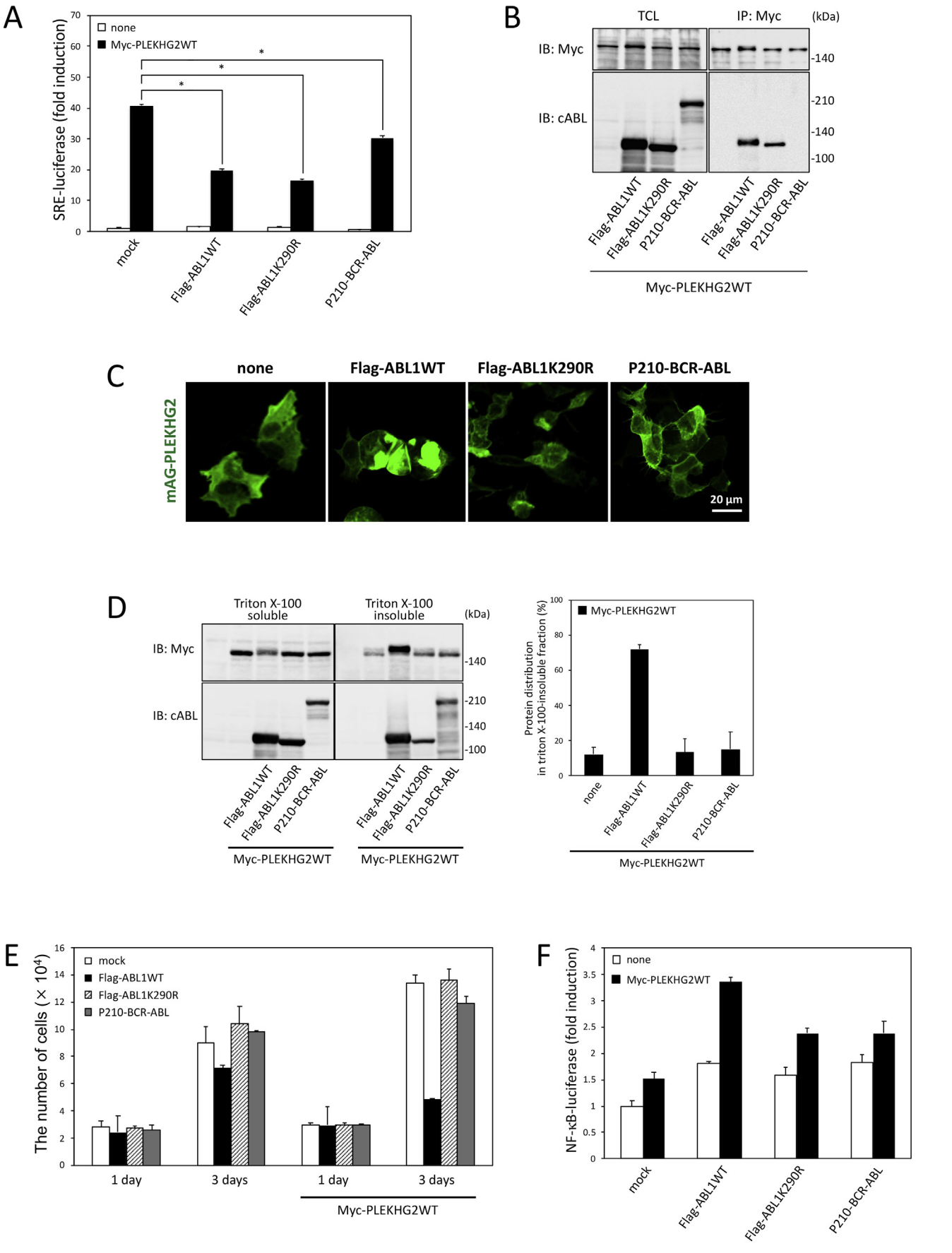

(caption on next page)

Fig. 6. Effects of the co-expression of PLEKHG2 and P210-BCR-ABL on cell functions.
(A) HEK293 cells were co-transfected with pSRE.L-luciferase, pRL-SV40, and expression vectors for Myc-PLEKHG2WT, Flag-ABL1WT, Flag-ABL1K290R and P210-BCR-ABL, as indicated. Luciferase activities were determined with a dual-luciferase reporter assay system and normalized for transfection efficiency, and the relative activities are shown when the value of mock was taken as 1.0. The experiment was performed in triplicate, and the values are the means ± S.D. (B) HEK293 cells were co-transfected with expression vectors for Myc-PLEKHG2WT, Flag-ABL1WT, Flag-ABL1K290R and P210-BCR-ABL, as indicated. Transfected cells were lysed 24 h after transfection, and immunoprecipitated with anti-Myc antibodies. Precipitated proteins were separated by SDS-PAGE and immunoblotted with anti-Myc antibody (for Myc-PLEKHG2WT) and anti-cABL antibody (for Flag-ABL1WT, Flag-ABL1K290R and P210-BCR-ABL). TCL, total cell lysate; IP, immunoprecipitation; IB, immunoblotting (C) HEK293 cells were co-transfected with expression vectors for mAG-tagged Myc-PLEKHG2WT, Flag-ABL1WT, Flag-ABL1K290R and P210-BCR-ABL, as indicated. Transfected cells were fixed and observed under a confocal laser scanning microscope. (D) HEK293 cells were co-transfected with expression vectors for Myc-PLEKHG2WT, Flag-ABL1WT, Flag-ABL1K290R and P210-BCR-ABL, as indicated. Transfected cells were fractionated into Triton X-100-soluble and -insoluble fractions. Fractionated proteins were separated by SDS-PAGE and immunoblotted with anti-Myc antibody (for Myc-PLEKHG2WT) and anti-cABL antibody (for Flag-ABL1WT, Flag-ABL1K290R and P210-BCR-ABL). The rate of band intensity of Myc-PLEKHG2, (Triton X-100 insoluble)/(Triton X-100 soluble + insoluble) (%), was quantitated as indicated. The data shown are representative of three independent experiments, and the values are the means ± S.D. IB, immunoblotting (E) HEK293 cells were co-transfected with expression vectors for Myc-PLEKHG2WT, Flag-ABL1WT, Flag-ABL1K290R, and P210-BCR-ABL, as indicated. The number of transfected cells was counted at 1 and 3 days after replating. The data shown are representative of three independent experiments, and the values are the means ± S.D. (F) HEK293 cells were co-transfected with pNF-κB-luciferase, pRL-SV40, and expression vectors for Myc-PLEKHG2WT, Flag-ABL1WT, Flag-ABL1K290R, and P210-BCR-ABL, as indicated. Luciferase activities were determined with a dual-luciferase reporter assay system and normalized for transfection efficiency, and the relative activities are shown when the value of mock was taken as 1.0. The experiment was performed in triplicate, and the values are the means ± S.D.

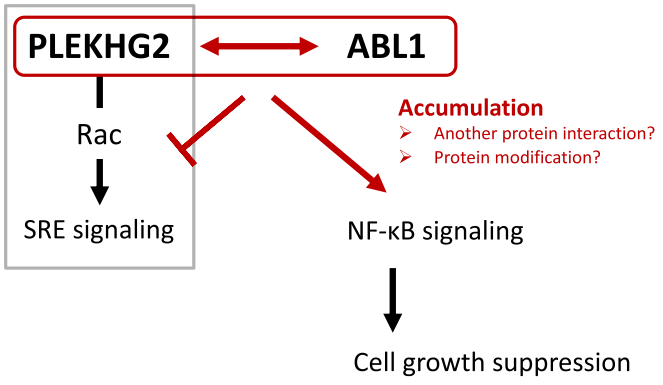

Fig. 7. Proposed cellular effects of the interaction between PLEKHG2 and ABL1. ABL1 attenuated PLEKHG2-induced serum response element-dependent gene transcription by the interaction between PLEKHG2 and ABL1. The co-expression of PLEKHG2 and ABL1 caused the formation of protein accumulation containing PLEKHG2 and ABL1 and suppressed cell growth through the NF-κB signaling pathway. Structural changes of PLEKHG2 and ABL1 by protein modification or another protein interaction may be required for the formation of the interaction between PLEKHG2 and ABL1.

either Myc-PLEKHG2 (1–464) or Myc-PLEKHG2 (465–1386) was also lower than the transcriptional activity level in cells co-expressing Flag-ABL1WT and Myc-PLEKHG2WT (Fig. 5H). These results suggest that the enhancement of NF-κB-dependent gene transcription relates to the accumulation of PLEKHG2 and ABL1. Therefore, we proposed that the PLEKHG2 and ABL1-induced intracellular protein accumulation drives cell growth suppression through NF-κB signaling.

3.6. Differential effects of BCR-ABL and ABL1 on PLEKHG2

It has been reported that the functions of ABL1 are involved in various disease states, including cancer [14,27]. For example, ABL1 can mediate tumor cell apoptosis and suppress tumor growth, but BCR-ABL which is the fusion protein produced in patients with Philadelphia chromosome-positive human leukemia as a result of chromosomal translocation of human ABL1 gene sequences on chromosome 9 to the breakpoint cluster region (BCR) gene sequences on chromosome 22 cannot. The BCR-ABL chimeric protein exhibits elevated tyrosine kinase and transforming activities, and has been identified in distinct human leukemias, including chronic myelogenous leukemia and acute lymphocytic leukemia [28–32]. It is also known that BCR-ABL utilizes Vav, a RhoGEF, to activate Rac signaling [33]. To investigate how ABL1 and BCR-ABL, two factors with clearly different functions, act on PLEKHG2, we examined their effects on the level of PLEKHG2-induced SRE-dependent gene transcription by ABL1WT and P210-BCR-ABL. The results showed that the attenuation of the level of PLEKHG2-induced SRE-dependent gene transcription in cells co-expressing Myc-PLEKHG2WT and P210-BCR-ABL was very weak compared to the attenuation in cells co-expressing Myc-PLEKHG2WT and either Flag-ABL1WT or Flag-ABL1K290R (Fig. 6A). Next, to examine whether there is a difference in the interaction with PLEKHG2 between ABL1 and BCR-ABL, we performed an immunoprecipitation experiment. The interaction of Myc-PLEKHG2WT with Flag-ABL1WT or Flag-ABL1K290R was detectable, but not that with P210-BCR-ABL (Fig. 6B). Next, we examined whether PLEKHG2 and BCR-ABL enhanced the intracellular protein accumulation. We found that the intracellular protein accumulation was detectable in the cells co-expressing Myc-PLEKHG2WT and Flag-ABL1WT, but not in those co-expressing Myc-PLEKHG2WT and Flag-ABL1K290R or P210-BCR-ABL (Fig. 6C). Analysis by subcellular fractionation using Triton X-100 further demonstrated that the amount of PLEKHG2 in the Triton X-100 insoluble fraction in cells co-expressing PLEKHG2WT and ABL1WT increased, but not that in cells co-expressing Myc-PLEKHG2WT and either Flag-ABL1K290R or P210-BCR-ABL (Fig. 6D). We then examined the effects of BCR-ABL on cell proliferation and the NF-κB-dependent gene transcription. The results of this analysis showed that the cell proliferation was suppressed in cells co-expressing Myc-PLEKHG2WT and Flag-ABL1WT, but not in cells co-expressing Myc-PLEKHG2WT and either Flag-ABL1K290R or P210-BCR-ABL (Fig. 6E). Similarly, NF-κB-dependent gene transcription was enhanced in cells co-expressing Myc-PLEKHG2WT and Flag-ABL1WT, but not in cells co-expressing Myc-PLEKHG2WT and either Flag-ABL1K290R or P210-BCR-ABL (Fig. 6F). These results suggested that BCR-ABL lacks the ability to suppress cell growth via NF-κB signaling, due to the weak interaction between PLEKHG2 and BCR-ABL.

4. Discussion

In this study, we demonstrated for the first time that ABL1 attenuated PLEKHG2-induced SRE-dependent gene transcription by the interaction of PLEKHG2 with ABL1 and that this interaction induces cell growth suppression through the NF-κB signaling pathway in HEK293 cells (Fig. 7).

It was previously reported that VAV1, a RhoGEF, was activated through its interactions with BCR-ABL and v-ABL via the SH3 domain [33]. In brief, the C-terminal SH3-SH2-SH3 domain of VAV1 interacted specifically with Bcr-Abl and v-Abl in a phosphotyrosine-dependent manner. In our recent study, PLEKHG2 phosphorylated by SRC interacted with PIK3R3 and ABL1 through the recognition of phosphotyrosine 489 in PLEKHG2 by the SH2 domain contained in PIK3R3 and ABL1 in EPHB2-stimulated cells [9]. On the other hand, several reports

have demonstrated that ABL phosphorylated and activated RhoGEFs including Sos-1, TRIO and Kalirin [16,17,34,35]. However, it is not known whether ABL1 regulated the activity of these RhoGEFs by interaction with them. In this study, we demonstrated that ABL1 attenuated PLEKHG2-mediated gene transcription by the interaction between PLEKHG2 and ABL1 in a phosphotyrosine-independent manner. In addition, our previous studies showed that β-actin and the heterotrimeric G protein Gαs subunit interacted with the region in the vicinity of the DH domain of PLEKHG2 and attenuated the PLEKHG2 activity [5,6]. From these reports, it is possible that ABL1 negatively regulates PLEKHG2 activity by causing structural changes near the DH domain of PLEKHG2 through a direct or indirect interaction.

In the present study, we found that PLEKHG2WT could not interact with ABL1WT, but PLEKHG2 (90–419) could interact with ABL1 (515–949) but not with ABL1 (515–749) in vitro. From results of immunoprecipitation experiments using cells expressing various mutants of PLEKHG2 and ABL1 and in vitro interaction experiments, it is suggested that amino acids 750 to 949 in ABL1 may be directly interacted to amino acids 90 to 150 in PLEKHG2. At the same time, these results suggested that the interaction between PLEKHG2 and ABL1 may require some structural change of PLEKHG2 and/or ABL1. It is possible that protein modification including phosphorylation and lipid modification and interaction with other proteins may cause these structural changes. There are several reports that ABL1 interacts several proteins including MEK kinase 1, CRK and the SRC kinase HCK [36–38]. Furthermore, it is known that ABL1 is regulated and tyrosine-phosphorylated by SRC [39]. In particular, SRC phosphorylates and interacts with PLEKHG2 (Fig. S2A) [9]. In the future, it is necessary to examine whether SRC is involved in intracellular protein accumulation by PLEKHG2 and ABL1, what kind of protein is included in this accumulation, and whether ABL1 or PLEKHG2 is modified within this accumulation.

In this study, we observed that the NF-κB signaling pathway played a key role in the accumulation of intracellular proteins and the suppression of cell growth by the interaction between PLEKHG2 and ABL1. A recent study showed that NF-κB activity is constitutively elevated in cAbl null fibroblasts [40]. Our present results suggested that the subcellular localization of ABL1 was changed by co-expression with PLEKHG2. One possible explanation for these findings is that ABL1 activity was locally decreased in cells, and this decrease induced the activation of NF-κB signaling. Another possibility suggested by our results is that the phosphorylation of proteins other than PLEKHG2 by ABL1 is necessary to the accumulation of PLEKHG2 and ABL1. A recent report showed that ABL1 interacts with, phosphorylates and co-localizes with C3G, a Rap-specific GEF that is co-localized in the cytoskeleton, and ABL1 induces apoptosis through a Rap1-triggered signaling pathway [41]. Rap1 is known to be an IκB kinase adaptor that regulates NF-κB-mediated gene transcription [42]. These facts raise the possibility of crosstalk between the ABL1-PLEKHG2-NF-κB signaling and ABL1-C3G-Rap1 signaling pathways. Further investigation of this point will be needed.

Finally, we revealed that the co-expression of PLEKHG2 with ABL1, but not BCR-ABL, suppressed cell growth and synergistically enhanced NF-κB-dependent gene transcription. It is well known that inhibitory intramolecular interactions of BCR-ABL are disrupted by BCR sequences, that BCR-ABL is constitutively tyrosine-phosphorylated, and that BCR-ABL is oligomerized by BCR sequences in cells [29,43]. It is considered that the structural alterations of ABL induced by the addition of BCR sequences—such as constitutive tyrosine phosphorylation and oligomerization—might weaken the interaction with PLEKHG2. On the other hand, the subcellular localization of ABL1 is also changed by the addition of BCR sequences, and it is considered that the protein phosphorylated by ABL1 also changes accordingly. Our results suggest that the phosphorylation of proteins other than PLEKHG2 by ABL1 may also be necessary for the accumulation induced by the interaction between PLEKHG2 and ABL1. There is also a possibility that BCR-ABL cannot phosphorylate the proteins required to induce the accumulation, because the subcellular localization or the substrate selectivity is changed by the addition of BCR sequences [32,44]. Further, three different BCR-ABL proteins that respectively contain P210, P185 and P230 and retain different numbers of BCR sequences have been identified and associated with distinct types of leukemia [43]. Since the effect of these fusion proteins on the function of PLEKHG2 may be different, it will also be necessary to study these fusion proteins in the future.

In summary, we have evaluated the cellular effects of the interaction between PLEKHG2 and ABL1 in HEK293 cells. Our data demonstrated that ABL1 attenuates PLEKHG2 functions by tyrosine-phosphorylated-independent interaction and induces intracellular protein accumulation in HEK293 cells. In particular, we provide evidence that the intracellular protein accumulated by the interaction of PLEKHG2 with ABL1 suppresses cell growth through the NF-κB signaling pathway.

Conflict of interests

The authors declare that they have no conflict of interest. All authors consented to participate, read the manuscript, and gave consent for publication. All data and materials are available for publication. No authors have competing interests.

Author contributions

MN, SN, HN, KS, YA, HN, HY, TN and HU designed the experiments; MN, SN, HN, KS, TS, and HY carried out the experiments; MN, SN, HN and HU carried out the statistical analyses; and MN, SN, HN, KS, TS, HN, HY, TN and HU wrote the manuscript. All authors approved the final version of the manuscript.

Acknowledgments

This study was supported by JSPS KAKENHI Grant Numbers 23590073 and 15K07927. The DNA sequence analysis was supported by the Division of Genomic Research of the Life Science Research Center at Gifu University.

Appendix A. Supplementary data

Supplementary data to this article can be found online at https://doi.org/10.1016/j.cellsig.2019.04.016.

References

[1] S. Etienne-Manneville, A. Hall, Rho GTPases in cell biology, Nature 420 (2002) 629–635, https://doi.org/10.1038/nature01148.
[2] K.L. Rossman, C.J. Der, J. Sondek, GEF means go: turning on RHO GTPases with guanine nucleotide-exchange factors, Nat. Rev. Mol. Cell Biol. 6 (2005) 167–180, https://doi.org/10.1038/nrm1587.
[3] S.M. Goicoechea, S. Awadia, R. Garcia-Mata, I'm coming to GEF you: regulation of RhoGEFs during cell migration, Cell Adhes. Migr. 8 (2014) 535–549, https://doi.org/10.4161/cam.28721.
[4] H. Ueda, R. Nagae, M. Kozawa, R. Morishita, S. Kimura, T. Nagase, O. Ohara, S. Yoshida, T. Asano, Heterotrimeric G protein betagamma subunits stimulate FLJ00018, a guanine nucleotide exchange factor for Rac1 and Cdc42, J. Biol. Chem. 283 (2008) 1946–1953, https://doi.org/10.1074/jbc.M707037200.
[5] K. Sugiyama, K. Tago, S. Matsushita, M. Nishikawa, K. Sato, Y. Muto, T. Nagase, H. Ueda, Heterotrimeric G protein Gαs subunit attenuates PLEKHG2, a rho family-specific guanine nucleotide exchange factor, by direct interaction, Cell. Signal. 32 (2017) 115–123, https://doi.org/10.1016/j.cellsig.2017.01.022.
[6] K. Sato, H. Handa, M. Kimura, Y. Okano, H. Nagaoka, T. Nagase, T. Sugiyama, Y. Kitade, H. Ueda, Identification of a rho family specific guanine nucleotide exchange factor, FLJ00018, as a novel actin-binding protein, Cell. Signal. 25 (2013) 41–49, https://doi.org/10.1016/j.cellsig.2012.09.015.
[7] K. Sato, M. Kimura, K. Sugiyama, M. Nishikawa, Y. Okano, H. Nagaoka, T. Nagase, Y. Kitade, H. Ueda, Four-and-a-half LIM domains 1 (FHL1) protein interacts with the rho guanine nucleotide exchange factor PLEKHG2/FLJ00018 and regulates cell morphogenesis, J. Biol. Chem. 291 (2016) 25227–25238, https://doi.org/10.1074/jbc.M116.759571.
[8] M. Nishikawa, K. Sato, S. Nakano, H. Yamakawa, T. Nagase, H. Ueda, Specific activation of PLEKHG2-induced serum response element-dependent gene

transcription by four-and-a-half LIM domains (FHL) 1, but not FHL2 or FHL3, Small GTPases (2017) 1–6, https://doi.org/10.1080/21541248.2017.1327838.
[9] K. Sato, T. Suzuki, Y. Yamaguchi, Y. Kitade, T. Nagase, H. Ueda, PLEKHG2/FLJ00018, a rho family-specific guanine nucleotide exchange factor, is tyrosine phosphorylated via the EphB2/cSrc signaling pathway, Cell. Signal. 26 (2014) 691–696, https://doi.org/10.1016/j.cellsig.2013.12.006.
[10] K. Sato, T. Sugiyama, T. Nagase, Y. Kitade, H. Ueda, Threonine 680 phosphorylation of FLJ00018/PLEKHG2, a rho family-specific guanine nucleotide exchange factor, by epidermal growth factor receptor signaling regulates cell morphology of neuro-2a cells, J. Biol. Chem. 289 (2014) 10045–10056, https://doi.org/10.1074/jbc.M113.521880.
[11] G.D. Kruh, R. Perego, T. Miki, S.A. Aaronson, The complete coding sequence of arg defines the Abelson subfamily of cytoplasmic tyrosine kinases, Proc. Natl. Acad. Sci. U. S. A. 87 (1990) 5802–5806, https://doi.org/10.1073/pnas.87.15.5802.
[12] J.Y.J. Wang, The capable ABL: what is its biological function? Mol. Cell. Biol. 34 (2014) 1188–1197, https://doi.org/10.1128/MCB.01454-13.
[13] S.E. Hernández, M. Krishnaswami, A.L. Miller, A.J. Koleske, How do Abl family kinases regulate cell shape and movement? Trends Cell Biol. 14 (2004) 36–44, https://doi.org/10.1016/j.tcb.2003.11.003.
[14] W.D. Bradley, A.J. Koleske, Regulation of cell migration and morphogenesis by Abl-family kinases: emerging mechanisms and physiological contexts, J. Cell Sci. 122 (2009) 3441–3454, https://doi.org/10.1242/jcs.039859.
[15] D.J. Forsthoefel, The Abelson tyrosine kinase, the Trio GEF and enabled interact with the netrin receptor frazzled in Drosophila, Development 132 (2005) 1983–1994, https://doi.org/10.1242/dev.01736.
[16] R. Kannan, J.-K. Song, T. Karpova, A. Clarke, M. Shivalkar, B. Wang, L. Kotlyanskaya, I. Kuzina, Q. Gu, E. Giniger, The Abl pathway bifurcates to balance enabled and Rac signaling in axon patterning in Drosophila, Development 144 (2017) 487–498, https://doi.org/10.1242/dev.143776.
[17] P. Sini, A. Cannas, A.J. Koleske, P.P. Di Fiore, G. Scita, Abl-dependent tyrosine phosphorylation of Sos-1 mediates growth-factor-induced Rac activation, Nat. Cell Biol. 6 (2004) 268–274, https://doi.org/10.1038/ncb1096.
[18] S.T. Wen, P.K. Jackson, R.A. Van Etten, The cytostatic function of c-Abl is controlled by multiple nuclear localization signals and requires the p53 and Rb tumor suppressor gene products, EMBO J. 15 (1996) 1583–1595 http://www.ncbi.nlm.nih.gov/pubmed/8612582%5Cnhttp://www.pubmedcentral.nih.gov/articlerender.fcgi?artid=PMC450068.
[19] J.G. Gong, A. Costanzo, H.Q. Yang, G. Melino, W.G. Kaelin, M. Levrero, J.Y. Wang, The tyrosine kinase c-Abl regulates p73 in apoptotic response to cisplatin-induced DNA damage, Nature 399 (1999) 806–809, https://doi.org/10.1038/21690.
[20] R. Agami, G. Blandino, M. Oren, Y. Shaul, Interaction of c-Abl and p73alpha and their collaboration to induce apoptosis, Nature 399 (1999) 809–813, https://doi.org/10.1038/21697.
[21] C.S. Hill, J. Wynne, R. Treisman, The rho family GTPases RhoA, Rac1, and CDC42Hs regulate transcriptional activation by SRF, Cell 81 (1995) 1159–1170, https://doi.org/10.1016/S0092-8674(05)80020-0.
[22] P.J. Woodring, T. Hunter, J.Y.J. Wang, Inhibition of c-Abl tyrosine kinase activity by filamentous actin, J. Biol. Chem. 276 (2001) 27104–27110, https://doi.org/10.1074/jbc.M100559200.
[23] E. Friederich, K. Vancompernolle, C. Huet, M. Goethals, J. Finidori, J. Vandekerckhove, D. Louvard, An actin-binding site containing a conserved motif of charged amino acid residues is essential for the morphogenic effect of villin, Cell 70 (1992) 81–92, https://doi.org/10.1016/0092-8674(92)90535-K.
[24] R. Parrondo, A. Pozas, T. Reiner, P. Rai, C. Perez-Stable, NF-κB activation enhances cell death by antimitotic drugs in human prostate cancer cells, Mol. Cancer 9 (2010) 182, https://doi.org/10.1186/1476-4598-9-182.
[25] M. Barkett, T.D. Gilmore, Control of apoptosis by Rel/NF-κB transcription factors, Oncogene 18 (1999) 6910–6924, https://doi.org/10.1038/sj.onc.1203238.
[26] F. Jin, X. Liu, Z. Zhou, P. Yue, R. Lotan, F.R. Khuri, L.W.K. Chung, S.-Y. Sun, Activation of nuclear factor-κB contributes to induction of death receptors and apoptosis by the synthetic retinoid CD437 in DU145 human prostate Cancer cells, Cancer Res. 65 (2005) 6354–6363, https://doi.org/10.1158/0008-5472.CAN-04-4061.
[27] A. Khatri, J. Wang, A.M. Pendergast, Multifunctional Abl kinases in health and disease, J. Cell Sci. 129 (2016) 9–16, https://doi.org/10.1242/jcs.175521.
[28] M. Wetzler, M. Talpaz, R.A. Van Etten, C. Hirsh-Ginsberg, M. Beran, R. Kurzrock, Subcellular localization of Bcr, Abl, and Bcr-Abl proteins in normal and leukemic cells and correlation of expression with myeloid differentiation, J. Clin. Invest. 92 (1993) 1925–1939, https://doi.org/10.1172/JCI116786.
[29] J.R. McWhirter, D.L. Galasso, J.Y. Wang, A coiled-coil oligomerization domain of Bcr is essential for the transforming function of Bcr-Abl oncoproteins, Mol. Cell. Biol. 13 (1993) 7587–7595, https://doi.org/10.1128/MCB.13.12.7587.Updated.
[30] G.Q. Daley, D. Baltimore, Transformation of an interleukin 3-dependent hematopoietic cell line by the chronic myelogenous leukemia-specific P210bcr/abl protein, Proc. Natl. Acad. Sci. U. S. A. 85 (1988) 9312–9316, https://doi.org/10.1073/pnas.85.23.9312.
[31] J. Zhu, J.Y.J. Wang, Death by Abl: a matter of location, Curr. Top. Dev. Biol. 59 (2004) 165–192, https://doi.org/10.1016/S0070-2153(04)59007-5.
[32] M. Koptyra, M. Nieborowska-Skorska, E.B. Gillespie, T. Stoklosa, G. Hoser, M. Wasik, M. Muschen, C. Richardson, T. Skorski, Normal ABL1 is a tumor suppressor and therapeutic target in BCR-ABL1–positive Leukemias, Blood 122 (2013) 2131–2144, https://doi.org/10.1182/blood-2015-11-681171.
[33] F. Bassermann, T. Jahn, C. Miething, P. Seipel, R.Y. Bai, S. Coutinho, V.L. Tybulewicz, C. Peschel, J. Duyster, Association of Bcr-Abl with the proto-oncogene Vav is implicated in activation of the Rac-1 pathway, J. Biol. Chem. 277 (2002) 12437–12445, https://doi.org/10.1074/jbc.M112397200.
[34] X.-M. Ma, M.B. Miller, K.S. Vishwanatha, M.J. Gross, Y. Wang, T. Abbott, T.T. Lam, R.E. Mains, B.A. Eipper, Nonenzymatic domains of Kalirin7 contribute to spine morphogenesis through interactions with phosphoinositides and Abl, Mol. Biol. Cell (2014), https://doi.org/10.1091/mbc.E13-04-0215.
[35] M. Sonoshita, Y. Itatani, F. Kakizaki, K. Sakimura, T. Terashima, Y. Katsuyama, Y. Sakai, M.M. Taketo, Promotion of colorectal cancer invasion and metastasis through activation of NOTCH–DAB1–ABL–RHOGEF protein TRIO, Cancer Discov. (2015), https://doi.org/10.1158/2159-8290.CD-14-0595.
[36] T. Yamauchi, G. Johnson, V. Kumar, P. Pandey, S. Kumar, A. Rana, M. Kaneki, L. Ghanem, Z.-M. Yuan, A. Bharti, S. Kharbanda, D. Kufe, R. Weichselbaum, Activation of MEK kinase 1 by the c-Abl protein tyrosine kinase in response to DNA damage, Mol. Cell. Biol. 20 (2002) 4979–4989, https://doi.org/10.1128/mcb.20.14.4979-4989.2000.
[37] S. Antoku, K. Saksela, G.M. Rivera, B.J. Mayer, A crucial role in cell spreading for the interaction of Abl PxxP motifs with Crk and Nck adaptors, J. Cell Sci. 121 (2008) 3071–3082, https://doi.org/10.1242/jcs.031575.
[38] S. Reis, M. Stanglmaier, M. Hallek, M. Warmuth, I. Kleinlein, The interaction of the Bcr-Abl tyrosine kinase with the Src kinase Hck is mediated by multiple binding domains, Leukemia 17 (2003) 283–289, https://doi.org/10.1038/sj.leu.2402778.
[39] A. Boureux, O. Furstoss, V. Simon, S. Roche, Abl tyrosine kinase regulates a Rac/JNK and a Rac/Nox pathway for DNA synthesis and Myc expression induced by growth factors, J. Cell Sci. 118 (2005) 3717–3726, https://doi.org/10.1242/jcs.02491.
[40] R.A. Liberatore, S.P. Goff, I. Nunes, NF-kappaB activity is constitutively elevated in c-Abl null fibroblasts, Proc. Natl. Acad. Sci. U. S. A. 106 (2009) 17823–17828, https://doi.org/10.1073/pnas.0905935106.
[41] A. Mitra, V. Radha, F-actin-binding domain of c-Abl regulates localized phosphorylation of C3G: role of C3G in c-Abl-mediated cell death, Oncogene 29 (2010) 4528–4542, https://doi.org/10.1038/onc.2010.113.
[42] H. Teo, S. Ghosh, H. Luesch, A. Ghosh, E.T. Wong, N. Malik, A. Orth, P. de Jesus, A.S. Perry, J.D. Oliver, N.L. Tran, L.J. Speiser, M. Wong, E. Saez, P. Schultz, S.K. Chanda, I.M. Verma, V. Tergaonkar, Telomere-independent Rap1 is an IKK adaptor and regulates NF-kappaB-dependent gene expression, Nat. Cell Biol. 12 (2010) 758–767, https://doi.org/10.1038/ncb2080.
[43] E.K. Greuber, P. Smith-Pearson, J. Wang, A.M. Pendergast, Role of ABL family kinases in cancer: from leukaemia to solid tumours, Nat. Rev. Cancer 13 (2013) 559–571, https://doi.org/10.1038/nrc3563.
[44] J. Voss, G. Posern, J.R. Hannemann, L.M. Wiedemann, A.G. Turhan, H. Poirel, O.A. Bernard, K. Adermann, C. Kardinal, S.M. Feller, The leukaemic oncoproteins Bcr-Abl and Tel-Abl (ETV6/Abl) have altered substrate preferences and activate similar intracellular signalling pathways, Oncogene 19 (2000) 1684–1690, https://doi.org/10.1038/sj.onc.1203467.